Research Article

NEURAL REGENERATION RESEARCH
www.nrronline.org

Chitosan alleviates symptoms of Parkinson's disease by reducing acetate levels, which decreases inflammation and promotes repair of the intestinal barrier and blood–brain barrier

Yinying Wang[1, 2, #], Rongsha Chen[1, #], Guolin Shi[3], Xinwei Huang[1], Ke Li[1], Ruohua Wang[1], Xia Cao[1], Zhongshan Yang[2, *], Ninghui Zhao[3, *], Jinyuan Yan[1, *]

https://doi.org/10.4103/NRR.NRR-D-23-01511

Date of submission: September 7, 2023

Date of decision: December 2, 2023

Date of acceptance: January 17, 2024

Date of web publication: June 26, 2024

From the Contents

Graphical Abstract

Chitosan activates the PPARD/AMPK pathway by reducing acetate levels to suppress inflammation, thereby repairing intestinal and blood–brain barriers, and alleviating Parkinson's disease symptoms

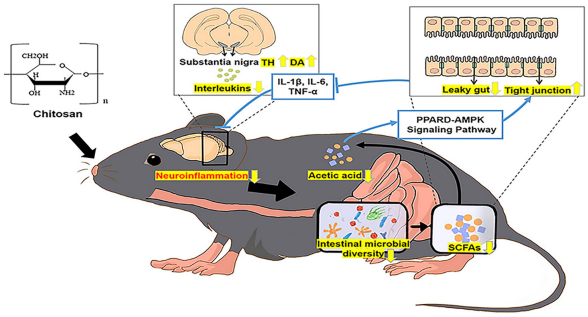

Abstract

Studies have shown that chitosan protects against neurodegenerative diseases. However, the precise mechanism remains poorly understood. In this study, we administered chitosan intragastrically to an MPTP-induced mouse model of Parkinson's disease and found that it effectively reduced dopamine neuron injury, neurotransmitter dopamine release, and motor symptoms. These neuroprotective effects of chitosan were related to bacterial metabolites, specifically short-chain fatty acids, and chitosan administration altered intestinal microbial diversity and decreased short-chain fatty acid production in the gut. Furthermore, chitosan effectively reduced damage to the intestinal barrier and the blood–brain barrier. Finally, we demonstrated that chitosan improved intestinal barrier function and alleviated inflammation in both the peripheral nervous system and the central nervous system by reducing acetate levels. Based on these findings, we suggest a molecular mechanism by which chitosan decreases inflammation through reducing acetate levels and repairing the intestinal and blood–brain barriers, thereby alleviating symptoms of Parkinson's disease.

Key Words: acetate; adenosine 5′-monophosphate-activated protein kinase; blood–brain barrier; chitosan; dopamine neurons; inflammation; intestinal barrier; Parkinson's disease; peroxisome proliferator-activated receptor delta; short-chain fatty acids

Introduction

Population aging lifespan extension have increased the prevalence of neurodegenerative diseases, especially Parkinson's disease (PD). PD is characterized by the degeneration of dopamine (DA) neurons in the substantia nigra and accumulation of α-synuclein (α-syn), and is accompanied by motor and non-motor symptoms, including kinesipathy, rigidity, tremors, cognitive impairment, sleep disorders, olfactory dysfunction, and constipation (Alarcón et al., 2023). PD can be treated with medication and deep brain stimulation; however, these therapies are not available, accessible, or affordable for all patients worldwide.

Polysaccharides are found in microorganisms, algae, plants, and animals and are highly bioactive. Polysaccharides such as cellulose and starch are degraded and absorbed, and their metabolites modulate host metabolism and pathophysiology. Other indigestible polysaccharides that cannot be hydrolyzed and absorbed may directly activate polysaccharide receptors or be metabolized by host intestinal microbes (Ahmadi et al., 2017). A recent study suggested that polysaccharides may play a role in neurodegenerative diseases (Wang et al., 2022b). Chitosan is a polysaccharide derived from deacetylated chitin. It can reduce mitochondrial damage and reactive oxygen species production, inhibiting apoptosis and increasing PC12 cell survival (Wang et al., 2016). Chitosan also suppresses mitochondrial dysfunction, nuclear condensation, and DNA fragmentation in a rotenone-induced cell model of PD (Manigandan et al., 2019). In addition, chitosan can be used deliver drugs

[1]Central Laboratory, The Second Affiliated Hospital of Kunming Medical University, Kunming, Yunnan Province, China; [2]Yunnan Provincial Key Laboratory of Molecular Biology for Sino Medicine, Yunnan University of Chinese Medicine, Kunming, Yunnan Province, China; [3]Department of Neurosurgery, The Second Affiliated Hospital of Kunming Medical University, Kunming, Yunnan Province, China

*Correspondence to: Zhongshan Yang, PhD, yangzhongshan@ynucm.edu.cn; Ninghui Zhao, MD, zhaoninghui@kmmu.edu.cn; Jinyuan Yan, PhD, yanjinyuan@kmmu.edu.cn. https://orcid.org/0000-0002-5270-0119 (Zhongshan Yang); https://orcid.org/0000-0002-1797-2071 (Ninghui Zhao); https://orcid.org/0000-0002-3398-3459 (Jinyuan Yan)

#Both authors contributed equally to this work and share first authorship.

Funding: *The study was supported by the National Natural Science Foundation of China, Nos. 32260196 (to JY), 81860646 (to ZY) and 31860274 (to JY); a grant from Yunnan Department of Science and Technology, Nos. 202101AT070251 (to JY), 202201AS070084 (to ZY), 202301AY070001-239 (to JY), 202101AZ070001-012, and 2019FI016 (to ZY).*

How to cite this article: *Wang Y, Chen R, Shi G, Huang X, Li K, Wang R, Cao X, Yang Z, Zhao N, Yan J (2026) Chitosan alleviates symptoms of Parkinson's disease by reducing acetate levels, which decreases inflammation and promotes repair of the intestinal barrier and blood–brain barrier. Neural Regen Res 21(1): 377-391.*

to the central nervous system (CNS) due to its strong permeability, mucus adhesion, biocompatibility, and degradability (Rassu et al., 2016; Yu et al., 2019; Chen et al., 2023; Liu et al., 2023). In animal models of PD, chitosan nanoparticles loaded with acteoside, the DA agonist rotigotin, or the protein phosphatase 2A activator FTY720 reduced α-syn aggregation and increased tyrosine hydroxylase (TH) expression, improving motor symptoms (Bhattamisra et al., 2020; Xue et al., 2020; Sardoiwala et al., 2021). Similarly, administration of chitosan-coated nanoemulsions of ropinirole and nigella oil minimized the toxicity of 6-hydroxydopamine and reversed behavioral symptoms in a rat model of PD (Nehal et al., 2021). These studies suggest that chitosan may protect against neuronal death in *in vitro* models or be an effective means of delivering medications in *in vivo* models. However, chitosan has poor blood–brain barrier (BBB) permeability and cannot be metabolized by humans, unless it is in nanoparticle form. Thus, the role of chitosan in PD requires further investigation.

In this study, we used cell and mouse models to explore the role of chitosan in PD. We found that chitosan lowers inflammation and repairs the intestinal barrier and the BBB, and elucidated the mechanism underlying these effects.

Methods

Animals and drug treatments

Female mice have a higher death rate and experience more side effects than male mice following MPTP exposure (Jackson-Lewis and Przedborski, 2007), so only male mice were used in this study. Male C57BL/6J mice (18–22 g, 8 weeks old) were obtained from the Animal Center, Kunming Medical University, China (license No. SCXK (Dian) K2020-0004). The Animal Ethics Committee of Kunming Medical University approved the study (approval No. kmmu20220443; approval date: February 21, 2022). All experiments were designed and reported according to Animal Research: Reporting of *In Vivo* Experiments (ARRIVE) guidelines (Percie du Sert et al., 2020). All mice were housed in a controlled, specific pathogen-free environment (temperature, 23 ± 3°C; humidity, 55% ± 15%, 12/12-hour light/dark cycle) with free access to food and water. Body weights were recorded daily. As shown in **Figure 1A**, the mice were randomly divided into seven groups: (1) the control group (n = 26), which received 125 μL normal saline via intraperitoneal injection once daily for 5 days; (2) the MPTP group (PD model group) (n = 26), which treated with MPTP-HCl (Sigma, St. Louis, MO, USA, M0896, 30 mg/kg) via intraperitoneal injection once daily for 5 days, followed by intragastric administration of 200 μL of 0.5% acetic acid (Tianjin Zhiyuan Chemical Reagent Co., Ltd., China) once daily for 26 days; (3) the MPTP + chitosan group (chitosan group) (n = 32), which was treated with same dosage of MPTP-HCl via intraperitoneal injection for 5 days, followed by intragastric administration of 200 μL of 0.5% chitosan (5 mg/mL, TCI, Tokyo, Japan, C0831) in 0.5% acetic acid once daily for 26 days; (4) the MPTP + chitosan + acetate [NaA]/butyrate [NaB]/propionate [NaP]/short-chain fatty acid [SCFAs] mixture group (NaA/NaB/NaP/SCFAs group) (n = 10 per group), which received the same treatment as the chitosan group, followed by oral administration of 67.5 mM sodium acetate (Sigma, S2889), 25 mM sodium propionate (Sigma, P1880), 40 mM sodium butyrate (Sigma, 303410), or a mixture of SCFAs (67.5 mM acetate, 40 mM butyrate, 25 mM propionate) for 28 days); (5) the control + NaA group (n = 4), which received the same treatment as the control group, followed by oral administration of 67.5 mM sodium acetate for 28 days; (6) the MPTP + NaA group (n = 4), which received the same treatment as MPTP group, followed by oral administration of 67.5 mM sodium acetate for 28 days; and (7) the peroxisome proliferator-activated receptor delta (PPARD) treatment group (n = 6), which received the same treatment as the chitosan group, followed by intragastric administration of 3 mg/kg GSK0660 (Selleck, Houston, TX, USA, S5817) for 28 days.

Cell culture and drug treatments

The human epithelial cell line Caco-2 was obtained from and identified by Kunming Institute of Zoology (Strok No. KCB200710YJ). The Caco-2 cell has been extensively used as a specialized model of intestinal epithelial cells *in vitro*, and accordingly, we selected it to investigate the role of acetate. The cells were maintained in Dulbecco's modified Eagle medium (Gibco, Suzhou, China, C11995500BT) supplemented with 10% fetal bovine serum (Gibco) and 1% penicillin/streptomycin (Gibco), and incubated under standard cell culture conditions (37°C, 5% CO_2). When the cells reached approximately 60%–70% confluency, they were treated with 500 μM sodium acetate, 20 μM of the PPARD agonist GW0742 (Selleck, S8020), 500 μM sodium acetate + 20 μM GW0742, 2 mM of the adenosine 5′-monophosphate-activated protein kinase (AMPK) agonist AICAR (MCE, Monmouth Junction, NJ, USA, HY-13417), or 500 μM sodium acetate + 2 mM AICAR. The Caco-2 cells were cultured for another 24 hours after drug treatment (**Figure 1B**).

Rotarod test

The rotarod test was performed using a five-lane rotarod apparatus (Jinan Yiyan Technology Development Co., Ltd, Jinan, China, YLS-4C) as described previously (Kumar et al., 2013), with some modifications. All mice were trained in advance on the rotarod apparatus for 3 consecutive days with accelerating speed (0 r/min to 30 r/min) over 300 seconds. Each mouse was then tested three times for 5 minutes each. The fall latency (time that elapsed before falling from the rod) was recorded for each mouse.

Western blotting

The mice were sacrificed by intraperitoneal injection with an overdose of 2% sodium pentobarbital (150 mg/kg, Ruitaibio, Beijing, China) (Laferriere and Pang, 2020), and the SN and colon were rapidly excised for protein extraction. Mouse SN and colon tissue or Caco-2 cells were homogenized on ice in radio immunoprecipitation assay lysis buffer (Beyotime, Shanghai, China, P0013B) containing protease inhibitor cOmplete Tablets, mini ethylene diamine tetraacetic acid-free, EASY pack (Roche, Basel, Switzerland, 04693159001). The homogenates were centrifuged at 13,000 × g for 15 minutes at 4°C, and the pellet was discarded. Next, 5× loading buffer (Epizyme, Shanghai, China, LT101S) was added to the supernatant, and the solution was boiled for 10 minutes. Then, the samples were run on 10%–12.5% sodium dodecyl sulphate-polyacrylamide gels (stacking gel: 70 V, separating gel: 90 V) and transferred to PVDF membranes (0.22 μm, Merck Millipore, Billerica, MA, USA, ISEQ00010) (transfer conditions: 90 V, on ice) using a Bio-Rad transfer apparatus (Bio-Rad, Mini-Protean Tetra System, Shanghai, China). The membranes were blocked with 5% non-fat milk for 2 hours, followed by overnight incubation with primary antibodies at 4°C. The primary antibodies used were as follows: rabbit anti-glyceraldehyde-3-phosphate dehydrogenase polyclonal antibody (GAPDH; 1:10,000, Proteintech, Wuhan, Hubei, China, Cat# 10494-1-AP, RRID: AB_2263076), rabbit anti-TH polyclonal antibody (1:5000, Proteintech, Cat# 25859-1-AP, RRID: AB_2716568), rabbit anti-zonula occludens-1 polyclonal antibody (ZO-1; 1:5000, Proteintech, Cat# 21773-1-AP, RRID: AB_10733242), rabbit anti-occludin polyclonal antibody (1:15,000, Proteintech, Cat# 27260-1-AP, RRID: AB_2880820), rabbit anti-AMPKα polyclonal antibody (1:1000, Cell Signaling Technology, Danvers, Massachusetts, USA, Cat# 2532, RRID: AB_330331), rabbit anti-phospho-AMPKα monoclonal antibody (1:1000, Cell Signaling Technology, Cat# 2535, RRID: AB_331250), and rabbit anti-PPARD polyclonal antibody (1:1000, Abcam, Cambridge, UK, Cat# ab23673, RRID: AB_2165902). Then, the membranes were washed three times with Tris-buffered saline containing Tween (TBST) and incubated with goat anti-KPL peroxidase-labeled affinity purified antibody to rabbit IgG (H + L) (1:10,000, KPL Affinity Purified Antibody, SeraCare, Milford, MA, USA, Cat# 5450-0010, RRID: AB_3075498) for 2 hours at 20–22°C. After washing the membranes three times, the protein bands were visualized by enhanced chemiluminescence (ECL, Beyotime, P0018FS). Images were analyzed using ImageJ v1.52a software (Schneider et al., 2012).

Quantitative polymerase chain reaction

Total RNA was extracted from colon tissue, SN tissue, and Caco-2 cells using TRIzol reagent (Ambion, Austin, TX, USA, 190903) according to the manufacturer's instructions. The extracted RNA was quantified using a NanoDrop2000 spectrophotometer (Thermo Fisher Scientific, Wilmington, DE, USA, NanoDrop ND-200), and all samples exhibited an $A_{260/280}$ ratio between 1.8 and 2.0. The RNA (1 μg) was then reverse transcribed into complementary DNA using a PrimeScript™ RT reagent kit containing gDNA Erase (Takara, Kyoto, Japan, RR047B), and quantitative polymerase chain reaction (QPCR) was performed using PowerUp™ SYBR™ Green Master Mix (Thermo Fisher Scientific, A25742). The primer sequences are shown in **Table 1**. mRNA levels were normalized to the housekeeping gene GAPDH and calculated using the $2^{-\Delta\Delta Ct}$ method (Livak and Schmittgen, 2001).

Enzyme-linked immunosorbent assay

The levels of interleukin (IL)-1β, IL-6, IL-10, and tumor necrosis factor (TNF)-α in plasma, as well as the levels of dopamine (DA) in feces, were determined by enzyme-linked immunosorbent assays (ELISAs) using kits from Jiangsu Meibiao Biotechnology Co., Ltd according to the manufacturer's instructions. Whole blood was collected from mice, and plasma was obtained using

Table 1 | **The primer sequences for QPCR used in this study**

Gene name	Species	Primer sequences (5'–3')
IL-1β	Human	Forward: CAG CCC ACA CAA GAA GGG TA
		Reverse: CTC TTC CTG GTT CAG CAC CC
IL-6	Human	Forward: CCT TCG GTC CAG TTG CCT T
		Reverse: AAG AGG TGA GTG GCT GTC TG
IL-8	Human	Forward: GGA TTG ATT GTC TGC TGG GGT
		Reverse: CAC CTC TCA CCA CTC AGG TC
IL-10	Human	Forward: CAC CTC CGC CAA TCT CTC AC
		Reverse: TCT TGG TTC TCA GCT TGG GG
TNF-α	Human	Forward: ATC CTG GGG GAC CCA ATG TA
		Reverse: AAA AGA AGG CAC AGA GGC CA
iNOS	Human	Forward: GAA CAA CGG CTC CAC ACT CA
		Reverse: TCA GCG AGC CGT AGT AGT TG
GAPDH	Human	Forward: ACA ACT TTG GTA TCG TGG AAG G
		Reverse: GCC ATC ACG CCA CAG TTT C
IL-1ß	Mouse	Forward: TGC CAC CTT TTG ACA GTG ATG
		Reverse: TGA TGT GCT GCT GCG AGA TT
IL-6	Mouse	Forward: GTC CTT CCT ACC CCA ATT TCC A
		Reverse: TGG TCT TGG TCC TTA GCC AC
IL-8	Mouse	Forward: CTG CGT CTT CAA CTT TCG CC
		Reverse: GCA CCA GTT TTC AAG GGG GA
IL-10	Mouse	Forward: GTG GAG CAG GTG AAG AGT GAT
		Reverse: AGT CCA GCA GAC TCA ATA CAC A
TNF-α	Mouse	Forward: TAG CCC ACG TCG TAG CAA AC
		Reverse: ACA AGG TAC AAC CCA TCG GC
iNOS	Mouse	Forward: CAG GGA GAA AGC GCA AAA CAT
		Reverse: CAT TCT GTG CTG TCC CAG TGA
SCD1	Mouse	Forward: TGG AGA CGG GAG TCA CAA GA
		Reverse: ACA CCC CGA TAG CAA TAT CCA G
SCD4	Mouse	Forward: AGC TGT CAC GCT CAT GTT CA
		Reverse: TAG AAG CAC AGC ATA CCG CA
PPARD	Mouse	Forward: GTC ATG GAA CAG CCA CAG GA
		Reverse: CGG AAG AAG CCC TGC ACA
FABP5	Mouse	Forward: AGA GCA CAG TGA AGA CGA CTG
		Reverse: ACC GTC TCA GTT TTT CTG CCA
FASN	Mouse	Forward: CTG CCT TCG GTT CAG TCT CTT
		Reverse: CAG AAT GGC ACA CCC TCC AA
GAPDH	Mouse	Forward: TGG CCT TCC GTG TTC CTA C
		Reverse: GAG TTG CTG TTG AAG TCG CA

FABP5: Fatty acid binding protein 5; FASN: fatty acid synthase; GAPDH: glyceraldehyde-3-phosphate dehydrogenase; IL-1β: interleukin-1 beta; IL-6: interleukin-6; IL-8: interleukin-8; IL-10: interleukin-10; iNOS: inductible nitric oxide synthase; PPARD: peroxisome proliferator activated receptor delta; QPCR: quantitative polymerase chain reactions; SCD1: stearoyl-coenzyme A desaturase 1; SCD4: stearoyl-coenzyme A desaturase 4; TNF-α: tumor necrosis factor alpha.

ethylene diamine tetraacetic acid anticoagulant (BD Biosciences, Franklin Lakes, NJ, USA, Cat# 367841); cerebrospinal fluid was collected from the cisterna magna of mice; and mouse feces sample were homogenized in 500 µL phosphate buffered saline (PBS). All the three samples above were centrifuged at 1118 × *g* for 20 minutes. Then, the supernatants from each of these samples were added to the antibody-precoated ELISA plate, 100 µL of HRP-conjugate reagent was added to each well, and the plates were incubated for 60 minutes at 37°C. Next, the wells were washed with washing buffer (200 µL/well) five times for 30 seconds each, followed by incubation in the dark with Chromogen Solution A (50 µL/well) and Chromogen Solution B (50 µL/well) for 15 minutes at 37°C. Finally, the reaction was stopped by adding 50 µL of stop solution to each well, and the absorbance was measured at 450 nm using a microplate reader (Thermo Fisher Scientific, Wilmington, DE, USA).

Immunofluorescence staining

For immunofluorescence staining, mice were sacrificed as described in the 'Western blotting' subsection. The perfused brains and colons with 4% paraformaldehyde were removed immediately and post-fixed for 24 hours in 4% paraformaldehyde, followed by cryoprotection in a 20% sucrose solution for at least 24 hours and storage in a 30% sucrose solution overnight at 4°C. The brains were cut into 30-µm–thick cryosections, and the colon tissue was cut into 15-µm–thick cryosections that were mounted on slides, which were then stored at –80°C. For immunofluorescence staining, the sections were washed with PBS three times for 5 minutes each and incubated with 1% normal goat serum for 1 hour at room temperature. Then, the slides were incubated overnight at 4°C with rabbit primary antibodies against: ionized calcium binding adaptor molecule 1 (Iba1; 1:2000, Abcam, Cat# ab178846, RRID: AB_2636859), ZO-1 (1:2000, Proteintech, Cat# 21773-1-AP, RRID: AB_10733242), and occludin (1:10,000, Proteintech, Cat# 27260-1-AP, RRID: AB_2880820). Next, they were incubated at 20–22°C for 2 hours with the corresponding fluorescent secondary antibody: Alexa Fluor 488 goat anti-rabbit lgG(H+L) (1:1000, Invitrogen, Cat# A11034, RRID: AB_2576217), Alexa Fluor 594 donkey anti-rabbit(H+L) (1:1000, Invitrogen, Cat# A21207, RRID: AB_141637), or Alexa Fluor 594 anti-TH (mouse, 1:500, Biolegend, Cat# 818003, RRID: AB_2801150). Subsequently, the slides were washed three times with PBS. Finally, 4′,6-diamidino-2-phenylindole (Abcam, ab104139) staining solution was added to the slides. Images were acquired using a fluorescence microscope (Olympus, Tokyo, Japan, BX51) equipped with a digital camera (Olympus, DP73) or a laser scanning confocal microscope (Olympus Biosystems, Hamburg, Germany, FV3000), and fluorescence intensity was analyzed using ImageJ software.

Evans blue staining

Evans blue (Sigma, 2% in normal saline) was injected intravenously (4 mg/kg) via the tail vein and allowed to circulate for 4 hours, after which the mice were sacrificed as described in the 'Western blotting' subsection. To evaluate blood–brain barrier (BBB) disruption, we utilized three different methods. In the first method, the brains were promptly removed and subsequently imaged using an *in vivo* bioluminescence imaging system (PerkinElmer, Waltham, MA, USA, IVIS Lumina III), and the images were analyzed using live image software (version 4.3; Caliper Life Sciences, Hopkinton, MA, USA) (excitation 658 nm and emission 719 nm). In the other two methods, BBB disruption was evaluated, as described previously (Do et al., 2014). In the second method, whole brains were weighed and placed in formamide at 60°C for 48 hours. Next, the homogenised samples with formamide were centrifuged for 20 minutes at 16,060 × *g*, the amount of Evans blue dye extracted from each brain was determined spectrophotometrically at 620 nm, and the volume of dye extravasation was calculated (Wei et al., 2013). The results were expressed as the total amount of Evans blue recovered, as compared with a standard curve. For the third method, brains were fixed in 4% paraformaldehyde in PBS, cryoprotected in a 20% sucrose solution, and stored in a 30% sucrose solution. The brain tissues were cut into 30-µm–thick slices that were mounted on slides, and images were acquired using a laser scanning confocal microscope. Evans blue dye appears red, and nuclear 4′,6-diamidino-2-phenylindole staining appears blue (Mendes et al., 2019).

Assessment of intestinal barrier integrity

Food was withheld from the mice for 12 hours, and the next day all mice were subjected to gavage with 200 µL of 6 mg/mL fluorescein isothiocyanate dextran (FITC-Dextran; Sigma, FD2000S; diluted in normal saline), which was allowed to circulate for 4 hours. Then, the mice were anesthetized with 2% pentobarbital sodium, blood was collected in heparinized tubes, serum was isolated, and the amount of FITC-dextran in the serum was determined by spectrophotometric analysis with an excitation peak at 480 nm and an emission peak at 520 nm.

16S rRNA gene sequence analysis of the intestinal microbiota

At least 100 mg of colonic contents were collected from control, MPTP mice, and chitosan mice, and the intestinal microbiota components were detected and quantified by Biomarker Technologies Company (Beijing, China) using full-length 16S sequencing. Briefly, total DNA was extracted from the samples using a PowerSoil® DNA Isolation kit (Tiangen Biochemical Technology Co., Ltd, Beijing, China, Cat# DP812). Next, polymerase chain reaction was carried out using 16S full-length primers, the reaction products were purified using AMpure PB Beads (Pacbio, Menlo Park, CA, USA), and the purified products were sequenced on a Sequel II (Pacbio) sequencer.

Gas chromatography-mass spectrometry analysis of SCFAs

Colon contents (> 100 mg), plasma (> 200 µL), and brain tissue (> 200 mg) were harvested, and their SCFA content was analyzed by BIOTREE Company (Shanghai, China) using gas chromatography-mass spectrometry. The SCFAs that were detected included acetic acid, propionic acid, butyric acid, valeric acid, hexanoic acid, isobutyric acid, and isovaleric acid.

Neurotransmitter measurement

Neurotransmitters, including DA and its metabolites, in the striatum of control, MPTP, and chitosan mice were measured by Biotree Company (Shanghai, China) using ultra-high performance liquid chromatography-MS/MS.

RNA sequencing

Colon tissue was harvested from mice, quickly immersed in 1.5 mL RNAlater, and stored overnight at 4°C. The next day, the colon tissue was transferred to –80°C for storage. Then, RNA sequencing analysis of the colon tissues was performed by Biomarker Technologies Company.

Hematoxylin-eosin staining

The frozen colon slices were removed from the –80°C freezer and thawed at 20–22°C, followed by rinsing twice with PBS. Then, the slices were stained with hematoxylin staining solution (Solarbio Technology Co., Ltd., Beijing, China, Cat# G1120) for 20 minutes, followed by washing with purified water for 30 seconds to remove any excess stain. Next, the tissues were stained with eosin staining solution for 2 minutes, rinsed with purified water, and soaked twice in ethanol (95%)–anhydrous ethanol-xylene for 1 minute each time. Finally, the slices were dried, sealed with neutral gum, and observed under a microscope (Olympus, Tokyo, Japan, BX51).

Statistical analysis

No calculation was performed to estimate the appropriate sample size, but the number of mice used was determined based on a previous study (Liu et al., 2020). All data are expressed as mean ± standard deviation (SD). Statistical analyses were performed using GraphPad Prism (version 9.3.1 for Windows, GraphPad Software, Boston, MA, USA, www.graphpad.com). Differences between groups were assessed by unpaired *t*-test, one-way analysis of variance, or two-way analysis of variance, followed by Tukey's multiple comparisons test. $P < 0.05$ indicated a significant difference.

Results

Chitosan alleviates motor dysfunction and protects dopamine neurons in an MPTP-induced mouse model of Parkinson's disease

Chitosan has neuroprotective effects in Drosophila melanogaster and PD cell models (Bhattamisra et al., 2020; Pramod Kumar and Harish Prashanth, 2020; Nehal et al., 2021; Sardoiwala et al., 2021); however, the mechanism by which chitosan exerts its neuroprotective effects in PD has not been elucidated, because it is indigestible *in vivo* (Gallaher et al., 2000; Yao and Chiang, 2006). As shown in **Figure 1C**, the average body weight was significantly lower in MPTP group than in the control group ($P < 0.0001$). By contrast, the average body weight in the chitosan treatment group was higher than that in the PD model group. Notably, mice exposed to MPTP exhibited motor dysfunction, while those that received oral administration of chitosan exhibited fewer symptoms (**Figure 1D**). DA neuron loss in the SN is the primary pathological characteristic of PD. TH is the rate-limiting enzyme in DA synthesis and a specific marker of DA neurons (Roy, 2017). We found that TH protein levels were significantly lower in MPTP-induced PD mice than in control mice ($P < 0.0001$); however, TH protein levels were partly restored in the chitosan treatment group ($P = 0.0042$; **Figure 1E**). Similarly, compared with the control group, there were fewer TH-positive cells in the SN in the MPTP model group; however, the animals treated with chitosan showed increased TH-positive cells by immunofluorescence staining (**Figure 1F**).

The death of DA neurons is accompanied by changes in the levels of DA and its primary metabolites, including 3,4-dihydroxyphenylacetic acid (DOPAC) and homovanillic acid (HVA), in the striatum (Yao et al., 2020). The DA content in the striatum of MPTP-induced PD mice was significantly lower than in control mice ($P = 0.0002$), and the DA content in the chitosan group was significantly higher than that in MPTP-induced PD mice ($P = 0.0046$; **Figure 1G**). Nevertheless, there was no significant difference in HVA and DOPAC levels among the three groups. The elevated DOPAC level and HVA/DA ratio in the striatum might be a compensatory mechanism for reduced DA neuron numbers and DA levels, as observed in patients with PD and in PD models (Pifl and Hornykiewicz, 2006). We calculated the DOPAC/DA, HVA/DA, and DOPAC + HVA/DA ratios as a proxy for DA utilization or metabolism. **Figure 1G** shows that the ratios of DOPAC/DA, HVA/DA, and DOPAC + HVA/DA ratios in MPTP-induced PD mice were significantly greater than those in control mice (DOPAC/DA: $P = 0.0125$; HVA/DA: $P = 0.0005$; DOPAC + HVA/DA: $P = 0.0006$). Oral administration of chitosan markedly decreased the DOPAC/DA and DOPAC + HVA/DA ratios (**Figure 1G**). These findings suggest that chitosan prevents motor dysfunction, facilitates DA neuron survival, increases DA content, and slows DA metabolism.

Chitosan reduces intestinal microbial diversity and short-chain fatty acid levels in an MPTP-induced mouse model of Parkinson's disease

Several lines of evidence suggest that polysaccharides are not broken down by saliva or gastrointestinal fluid because of a lack of appropriate enzymes, but can be partially or fully hydrolyzed by the intestinal microbiota (El Kaoutari et al., 2013). Because chitosan cannot be digested by humans, it may regulate the intestinal flora and the production of metabolites, including SCFAs, trimethylamines, amino acid derivatives, and vitamins (Uyanga et al., 2023). Therefore, we analyzed the mouse intestinal microbiota by performing 16S rDNA sequencing of feces to determine how chitosan improves PD symptoms. Microbiota complexity can be described by α- and β-diversity (Singh et al., 2023). A heat map was obtained to display the top 30 bacterial genera (**Figure 2A**). The MPTP-induced PD mice treated with chitosan demonstrated altered intestinal microbiota composition (**Figure 2B–D**). A Venn diagram of the gut microbes (**Figure 2B**) displays the operational taxonomic unit distribution in the three groups including the control, MPTP, chitosan. The three groups shared 109 operational taxonomic units, and 3, 5, and 11 operational taxonomic units were unique to the control, MPTP, and MPTP + chitosan groups, respectively (**Figure 2B**). Chao1, Shannon, and Simpson indices were used to describe the α-diversity, which was used to evaluate the species richness and evenness (Wang et al., 2022a). The Shannon ($P = 0.0343$) and Simpson ($P = 0.0337$) indices were significantly elevated in the PD model group, whereas the Shannon ($P = 0.0211$) and Simpson ($P = 0.0293$) indices in chitosan-treated mice showed a significant decreasing trend (**Figure 2C**). Principal coordinate analysis measures β-diversity and is used to assess differences or similarities in microbiota communities (Wang et al., 2022a). The principal coordinate analysis score plot (ANOSIM $R = 0.61$, $P = 0.001$) revealed that the three groups were significantly distinct in terms of microbiota community structure (**Figure 2D**). The chitosan precursor chitin is a component of fungal cell walls (Brown et al., 2020). We detected intestinal fungi using ITS sequencing and found no change in fungal abundance or composition in MPTP-induced mice treated with chitosan compared with the MPTP group (**Additional Figure 1A–D**). To determine whether the increase in DA content in the striatum occurred because of changes in the intestinal microbiota, we measured DA levels in mouse feces and found no significant differences among the groups (**Additional Figure 1E**). These findings demonstrated that treatment with chitosan can alter microbiota composition and reduce gut flora diversity in MPTP-induced PD mice.

To further investigate the role of intestinal microbiota and their metabolites, we measured the levels of SCFAs which are produced by gut microorganisms through the fermentation of undigested and unabsorbed carbohydrates, including acetate, propionate, butyrate, valerate, caproate, isobutyrate, and isovalerate, using gas chromatography–mass spectrometry. We found that MPTP-induced PD mice had higher concentrations of SCFAs than control mice. Acetate ($P = 0.0071$), propionate ($P = 0.0023$), and valerate ($P = 0.0001$) levels were significantly higher in the MPTP group than in the control group (**Figure 2E**). By contrast, acetate ($P = 0.0005$), propionate ($P = 0.0001$), butyrate ($P = 0.0131$), and valerate ($P = 0.0008$; **Figure 2E**) levels were significantly lower in the chitosan treatment group than in the MPTP group. We also measured SCFAs in plasma and found no differences between untreated mice and those treated with chitosan (**Figure 2F**). Interestingly, a previous study observed opposite changes in feces and plasma SCFA levels in patients with inflammatory bowel disease characterized by increased intestinal permeability (Jaworska et al., 2019). Yang et al. (2022) reported synchronously decreased fecal SCFA levels and increased plasma SCFA levels in a large sample of patients with PD, suggesting that plasma SCFA levels result from increased penetration from the gut to the blood or increased gut–blood barrier (GBB; also called as intestinal barrier) permeability; therefore, the ratio of plasma SCFA levels to feces SCFA levels was used as a marker of GBB permeability. SCFAs can cross the BBB to interact with microglia and regulate brain function; therefore, we further investigated SCFA levels in mouse brains. Of note, there were no significant differences in MPTP and chitosan (**Figure 2G**). Hence, SCFAs may not directly act on the brain in PD. Taken together, our findings suggest that chitosan modulates the structure of the microbial community in the gut, reducing bacterial diversity and SCFA levels in mouse feces, but does not change SCFA levels in the plasma or brain.

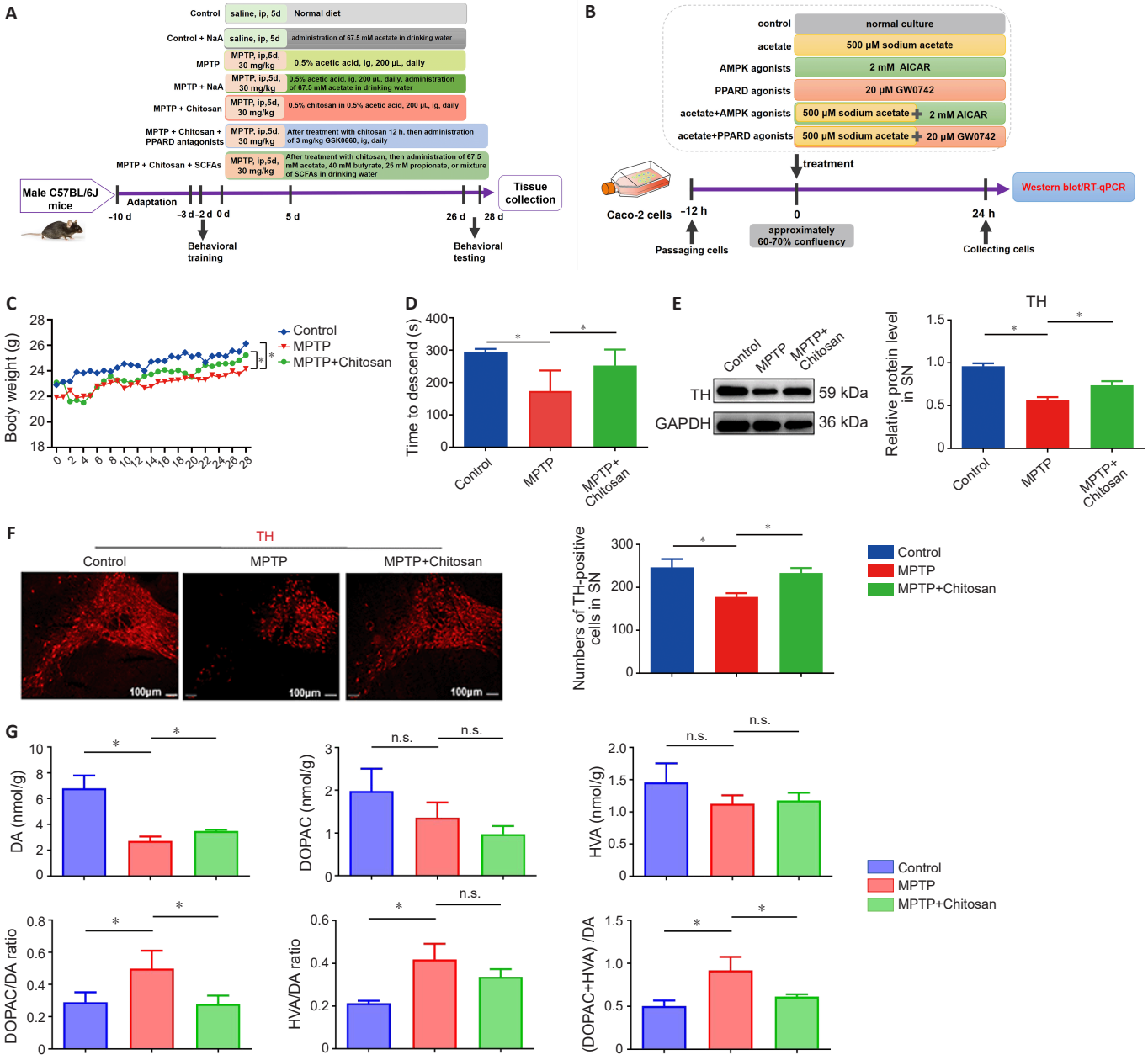

Figure 1 | **Chitosan alleviates motor dysfunction and improves DA neuron survival in an MPTP-induced mouse model of PD.**

(A) Experimental timeline of behavioral tests and sample collection from the different treatment groups, including control, NaA alone, MPTP-induced PD model, MPTP + NaA, chitosan treatment, MPTP + chitosan + PPARD antagonist, and SCFA treatment. (B) Experimental timeline of cell treatment with acetate, an AMPK agonist, and a PPARD agonist. (C) Chitosan significantly increased mouse body weight (n = 7/group). (D) In the rotarod test, fall latency was increased after chitosan treatment (n = 7/group). (E) Chitosan administration significantly increased TH expression, as determined by western blot assay. GAPDH was used as loading control (n = 3/group). (F) Chitosan treatment significantly increased the number of TH-positive dopaminergic neurons (red, Alexa Fluor 594), as determined by immunofluorescence staining (n = 3/group). Scale bars: 100 μm. (G) UHPLC-MS/MS was used to detect DA, DOPAC, and HVA levels in striatum tissue (n = 4/group). Treatment with chitosan significantly upregulated the levels of DA, DOPAC/DA, and (DOPAC + HVA)/DA, but there was no significant change in HVA/DA levels. All data are presented as the mean ± SD. All experiments were repeated at least three times. *P < 0.05 (two-way analysis of variance followed by Tukey's multiple comparisons test (C) or one-way analysis of variance followed by Tukey's multiple comparisons test (D–G). AMPK: Adenosine 5′-monophosphate-activated protein kinase; DA: dopamine; DOPAC: 3,4-dihydroxyphenylacetic acid; GAPDH: glyceraldehyde-3-phosphate dehydrogenase; HVA: homovanillic acid; ig: intragastrical administration; ip: intraperitoneal administration; MPTP: 1-methyl-4-phenyl-1,2,3,6-tetrahydropyridine; n.s.: no significance; NaA: sodium acetate; PD: Parkinson's disease; PPARD: peroxisome proliferator-activated receptor delta; SCFA: short-chain fatty acid; SN: substantia nigra; TH: tyrosine hydroxylase.

Chitosan restores the integrity of the damaged intestinal barrier and blood–brain barrier in an MPTP-induced mouse model of Parkinson's disease

It is unclear how chitosan alleviates PD symptoms by inhibiting SCFA production in the gut. Recent clinical and laboratory studies have shown that PD disrupts the intestinal barrier (Dong et al., 2020; Yang et al., 2022). Because the primary site of chitosan action after ingestion is the intestine, we first asked whether chitosan alters intestinal function. To test whether chitosan alleviates PD symptoms by repairing the intestinal barrier, we measured the expression levels of the tight junction proteins ZO-1 and occludin, which are necessary for barrier function and integrity (Wu et al., 2000). We found that ZO-1 and occludin were expressed at lower levels in the MPTP group than in the control group, whereas the expression of both proteins was upregulated in the chitosan treatment group (**Figure 3A**). The ZO-1 and occludin fluorescence intensity results were confirmed by western blotting (**Figure 3B**). Next, FITC-dextran was used to evaluate intestinal barrier permeability. Under normal conditions, FITC-dextran cannot cross the epithelial barrier. When the intestinal barrier is disrupted due to inflammation, it can be crossed by FITC-dextran (Baxter et al., 2017). A significant increase in FITC-dextran in the serum of MPTP-induced PD mice was observed relative to the control group (P = 0.0078); however, treatment with chitosan decreased serum FITC-dextran levels compared with the MPTP group, suggesting that MPTP-induced PD mice have high intestinal permeability (**Figure 3C**).

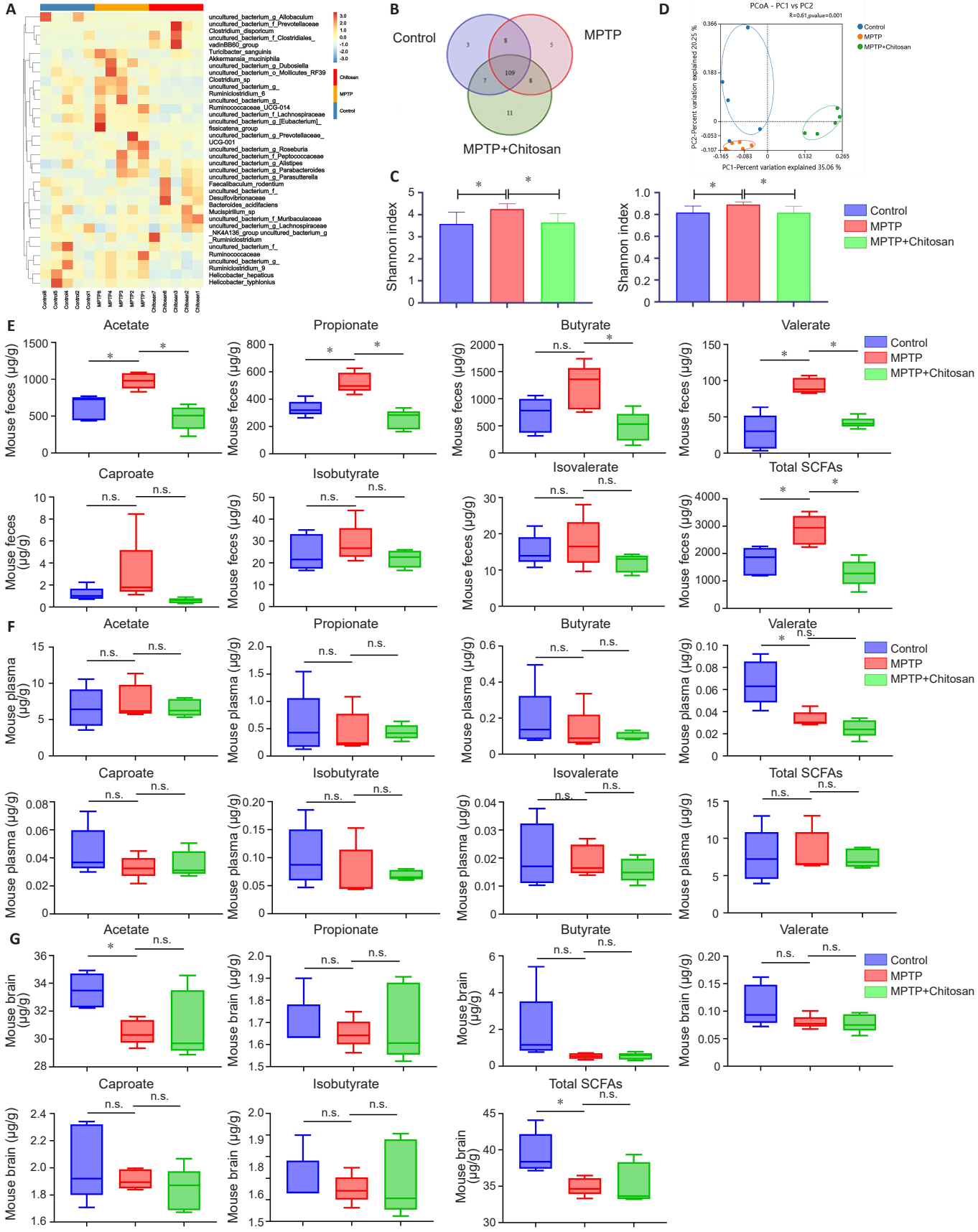

Figure 2 | **Chitosan reduces intestinal microbial diversity and SCFA concentrations in the feces of an MPTP-induced mouse model of PD.**

(A) Heatmap of 16S rRNA gene sequencing analysis of feces at the species level. (B) Venn diagram of DEGs in mouse feces showing the number of shared and unique genes for each group. (C) α-Diversity (Shannon index and Simpson index) depicted in boxplots. Chitosan treatment significantly decreased the α-diversity compared with the MPTP group. (D) β-Diversity analysis visualized as PCoA plots. (E) GC-MS was used to detect SCFA concentration in mouse feces. Chitosan treatment significantly decreased total SCFA levels compared with the MPTP group, and acetic acid, propionic acid, butyric acid, and valeric acid levels decreased most significantly. (F, G) Chitosan treatment did not alter SCFA concentrations in the plasma or brain in all three groups. All data are presented as the mean±SD (n = 5/group). *P < 0.05 (unpaired t-test [C] or one-way analysis of variance followed by Tukey's multiple comparisons test [E–G]). DEGs: Differentially expressed genes; GBB: gut–blood barrier; GC-MS: gas chromatography-mass spectrometer; MPTP: 1-methyl-4-phenyl-1,2,3,6-tetrahydropyridine; n.s.: no significance; PCoA: principal coordinates analysis; PD: Parkinson's disease; SCFA: short-chain fatty acid.

Next, we asked whether damage to the intestinal barrier would lead to BBB damage. Evans blue is widely used to evaluate BBB integrity (Xu et al., 2019). The MPTP-induced PD mice exhibited significantly increased BBB leakage compared with control mice (P = 0.0089), and treatment with chitosan reduced BBB leakage (**Figure 3D**). BBB leakage was also measured in brain sections by fluorescence microscopy, which showed that the Evans blue fluorescence intensity was significantly higher in the MPTP group than in the control group, and that treatment with chitosan significantly reversed this effect (**Figure 3E**). Next, we confirmed these results by soaking brain tissue in formamide, which is a solvent for Evans blue (Lima et al., 2023), and calculating the brain content of Evans blue based on a standard curve. Consistent with the microscopy results, the formamide quantification results showed that the Evans blue level was significantly elevated (P = 0.0384) in the brains of MPTP-induced PD mice compared with the control mice and decreased following chitosan administration compared with MPTP mice (P = 0.0351; **Figure 3F**). These results suggest that chitosan may restore damage to the intestinal barrier and the BBB, thereby exerting a therapeutic effect in MPTP-induced PD mice.

Chitosan alleviates motor dysfunction and protects dopamine neurons by reducing acetate

To confirm that chitosan alleviates PD symptoms by decreasing SCFA levels, we supplemented the animals' drinking water with 67.5 mM NaA, 25 mM NaP, 40 mM NaB, and mixed SCFAs (Smith et al., 2013). As shown in **Figure 4A**, the body weights of the PD mice were significantly lower than those of the control animals (P < 0.0001), while chitosan treatment was associated with weight gain (P < 0.0001). Meanwhile, the mice consuming mixed SCFAs exhibited significantly lower weights than the MPTP + chitosan mice (P < 0.0001; **Figure 4A**). The MPTP-induced PD mice also demonstrated a significant decrease in fall latency in the rotarod test compared with the control group, while mice treated with chitosan showed improved motor performance (**Figure 4B**). Compared with the MPTP + chitosan group, the mice that received acetate and mixed SCFAs exhibited significant motor impairment (**Figure 4B**). Next, we assessed whether SCFAs would reduce the damage to DA neurons, by western blotting and immunofluorescence. Compared with the model group, the chitosan treatment group exhibited higher TH levels. In contrast, acetate, propionate, and mixed SCFAs lowered TH protein levels to PD model levels (**Figure 4C**). Acetate (P = 0.0003), propionate (P = 0.0093), and mixed SCFAs (P = 0.0093) significantly accelerated DA neuron (TH-positive cell) loss (**Figure 4D**). These findings suggest that NaA, NaP, and mixed SCFAs reversed the protective effect of chitosan. We also investigated whether acetate would have a negative effect on control and PD model mice. Brain section analysis showed no difference in the number of TH-positive neurons in the SN between control mice with or without NaA, indicating that NaA did not

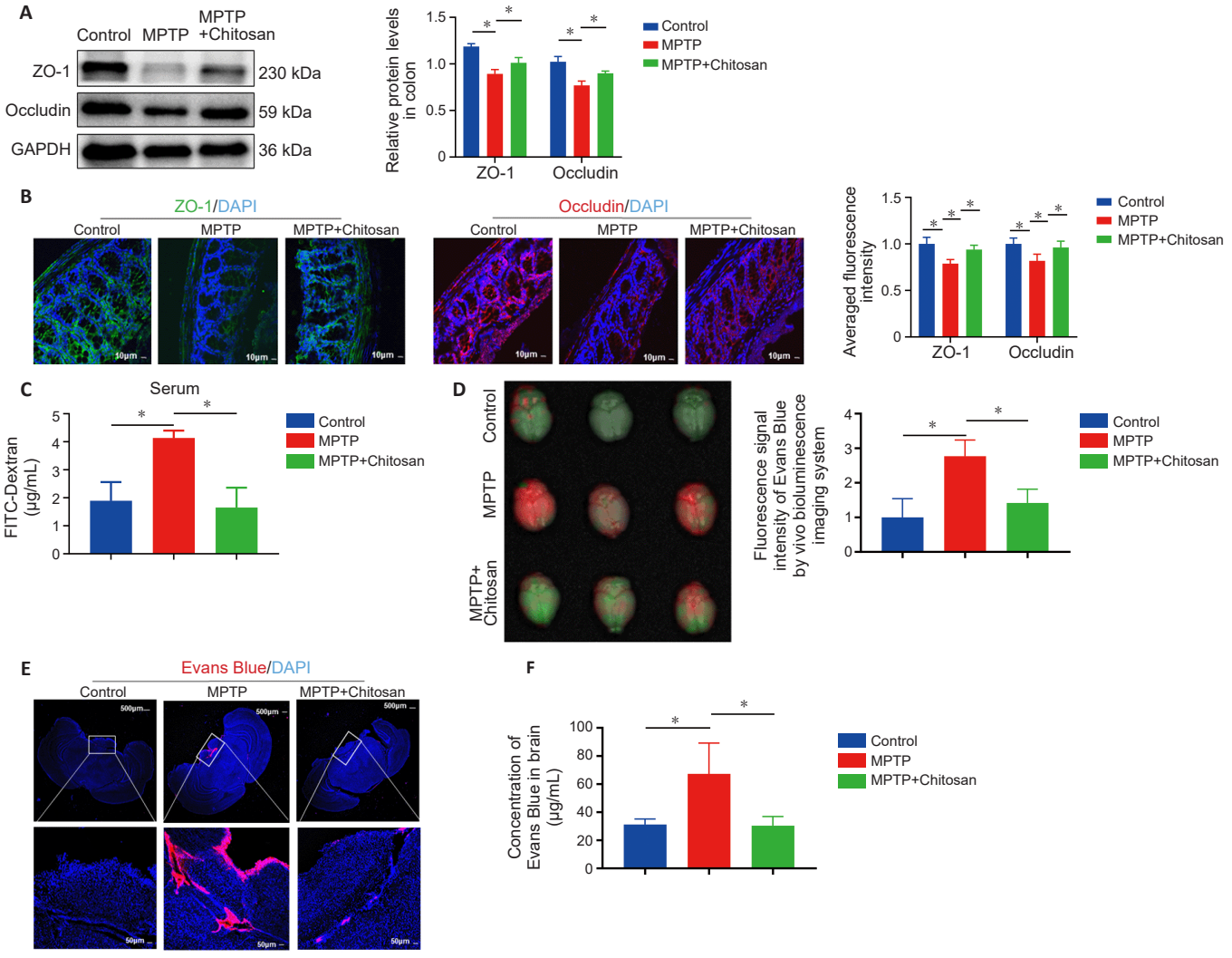

Figure 3 | **Chitosan treatment repairs damaged intestinal and blood–brain barriers in an MPTP-induced mouse model of PD.**

(A) Chitosan administration significantly increased ZO-1 and occludin expression levels, as detected by western blot. GAPDH was used as a loading control. (B) Chitosan treatment significantly increased the fluorescence intensity of ZO-1 (green, Alexa Fluor 488) and occludin (red, Alexa Fluor 594) in mouse colon tissue compared with the MPTP-induced PD group, and the fluorescence intensities of ZO-1 and occludin in PD group were lower than those in the control group. Scale bars: 10 μm. (C) Compared with MPTP-induced PD mice, chitosan treatment significantly decreased serum FITC-dextran levels, which are a measure of intestinal barrier integrity. (D) EB was used to monitor BBB permeability, and results were normalized to the control group. Chitosan treatment significantly reduced BBB damage. (E) EB measured by fluorescence microscopy imaging. Chitosan significantly restored BBB compared with MPTP-induced PD mice. Scale bars: 500 μm (upper) and 50 μm (lower). (F) EB of brain in mice measured by microplate reader. Chitosan treatment significantly decreased EB content compared with MPTP mice. All data are presented as the mean ± SD (n = 3/group). *P < 0.05 (one-way analysis of variance followed by Tukey's multiple comparisons test). BBB: Blood–brain barrier; DAPI: 4′,6-diamidino-2-phenylindole; EB: Evans blue; FITC-Dextran: Fluorescein isothiocyanate dextran; GAPDH: glyceraldehyde-3-phosphate dehydrogenase; MPTP: 1-methyl-4-phenyl-1,2,3,6-tetrahydropyridine; PD: Parkinson's disease; ZO-1: Zonula occludens-1.

affect control mice (**Additional Figure 2A–C**). Similarly, the number of TH-positive cells in the MPTP group exposed to NaA decreased compared with the MPTP group, but the difference was not significant. We speculate that this is because the loss of DA neurons induced by MPTP was so severe that any additional DA neuron loss caused by NaA was not evident. In addition, hematoxylin-eosin staining showed that colon tissue in the control + NaA group was structurally intact and contained few infiltrating inflammatory cells, and there was no difference between the control group and the control + NaA group (**Additional Figure 2D**). The QPCR analysis results were consistent with the hematoxylin-eosin staining results, in that the relative mRNA levels of IL-1β and IL-6 in the colon tissue of control + NaA mice were comparable to those seen in the control mice (**Additional Figure 2E**). Therefore, we explored acetate further in subsequent experiments, as it appeared to cause motor impairment and DA neuron loss.

Acetate damages the intestinal barrier and triggers inflammation in an MPTP-induced mouse model of Parkinson's disease

SCFAs interact locally with intestinal epithelial cells to mediate intestinal mucosal immunity and barrier function (Dalile et al., 2019). As described above, we found that chitosan treatment restored intestinal barrier integrity (**Figure 4**). Colon length is a marker for evaluating the severity of colonic inflammation (Tanaka et al., 2003). We observed no significant difference in colon length among the groups including the control, MPTP, chitosan and chitosan + NaA groups (**Figure 5A**). ZO-1 and occludin protein levels were elevated in the chitosan group than MPTP group; however, acetate supplementation was associated with a decreasing trend in the expression of these two proteins (**Figure 5B**). Likewise, immunofluorescence analysis of colon sections showed that ZO-1 and occludin expression levels were lower in the acetate group than in the chitosan group (**Figure 5C**). These findings suggest that acetate suppresses ZO-1 and occludin expression, thereby damaging the mouse intestinal barrier.

It remains unclear how disruption of the intestinal barrier aggravates PD. Talley et al. (2021) reported that local inflammation in the colon drives systemic inflammation and neuroinflammation through the gut–brain signaling axis, potentially mediated by the gut microbiota; alternatively, inflammation in the intestine could lead to systemic inflammation and subsequently activate CNS inflammation. To explore the effect of acetate supplementation on inflammation following chitosan treatment, we measured changes in inflammatory factors in the colon, plasma, and SN. Levels of the pro-inflammatory factors IL-1β, IL-6, IL-8, TNF-α, and iNOS were elevated in the colon in MPTP group compared with the control group. The expression level of the anti-inflammatory cytokine IL-10 in the colon was lower in MPTP mice than in control mice (**Figure 5D**). Compared with the MPTP group, mice treated with chitosan showed lower IL-1β, IL-8, and TNF-α expression levels in the colon, but no significant changes in IL-6, IL-10, or iNOS expression levels (**Figure 5D**). However, acetate supplementation increased IL-1β, IL-6, TNF-α, and iNOS expression in the colon (**Figure 5D**). SCFAs affect systemic inflammation by regulating interleukin secretion (Dalile et al., 2019). Mice in the MPTP group exhibited higher plasma IL-1β and TNF-α levels than control mice (**Figure 5E**), while chitosan treatment significantly reduced IL-1β (P = 0.0128) and TNF-α (P = 0.0003) levels and increased IL-10 (P = 0.0002) levels

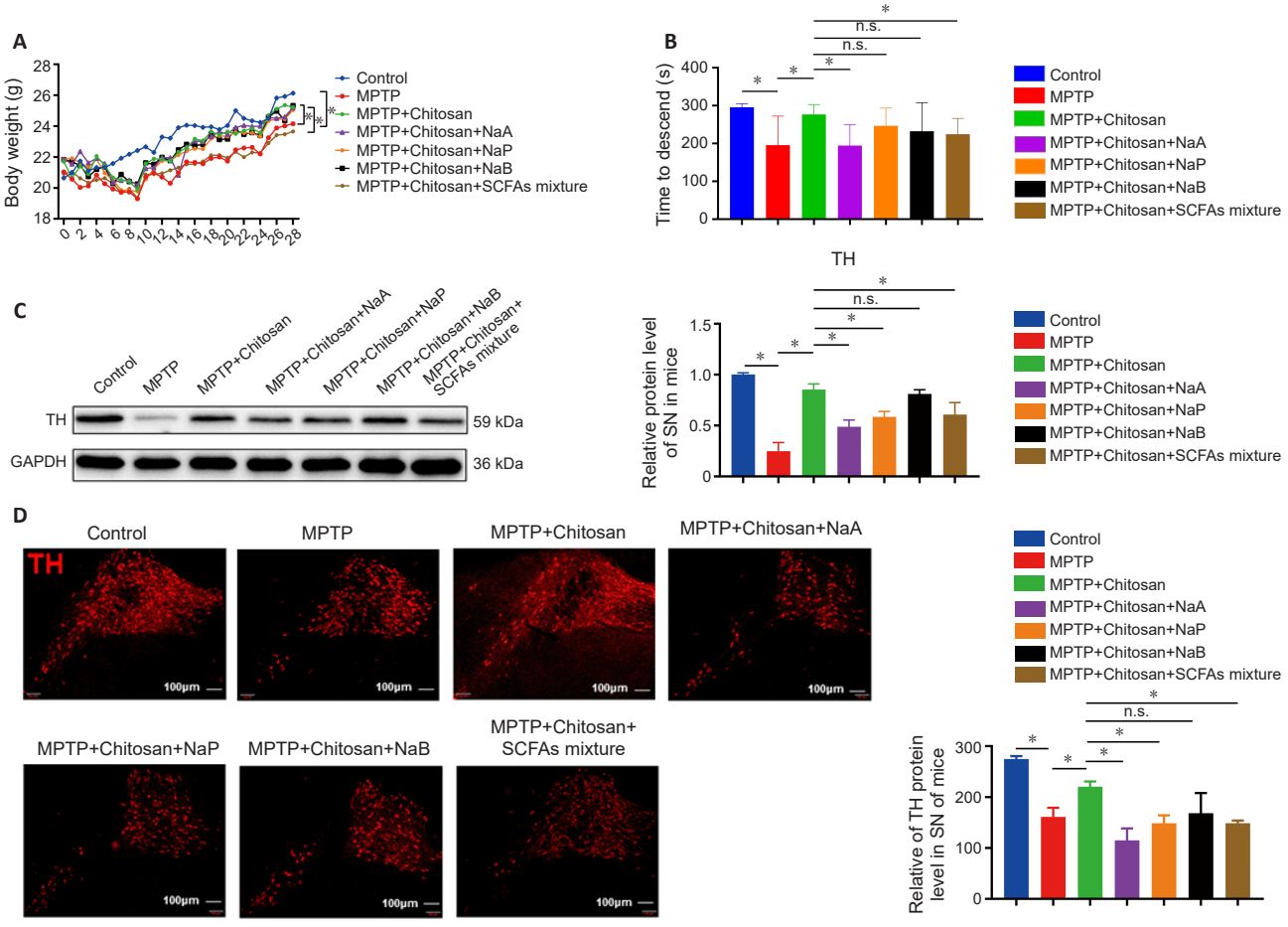

Figure 4 | **Acetate supplementation decreases the number of DA neurons in an MPTP-induced mouse model of PD.**
(A) Body weights in the different groups (n = 10/group). (B) Administration of acetate and mixed SCFAs increased motor dysfunction relative to the chitosan group (n = 10/group). The fall latency in chitosan treatment group was longer than that in the MPTP group, but the fall latency in the acetate and mixed SCFAs supplementation group was shorter than that in the chitosan group. (C) Compared with the chitosan group, supplementation with acetate, propionate, and mixed SCFAs decreased TH expression (normalized to the control group), as determined by western blot (n = 3/group). GAPDH was used as a loading control. (D) Administration of acetate, propionate, and mixed SCFAs significantly decreased the number of TH-positive dopaminergic neurons (red, Alexa Fluor 594) compared with the chitosan group, as detected by immunofluorescence staining (n = 3/group). Scale bars: 100 μm. All data are presented as the mean ± SD. All experiments were repeated at least three times. *P < 0.05 (two-way analysis of variance followed by Tukey's multiple comparisons test [A] or one-way analysis of variance followed by Tukey's multiple comparisons test [B–D]). DA: Dopamine; GAPDH: glyceraldehyde-3-phosphate dehydrogenase; MPTP: 1-methyl-4-phenyl-1,2,3,6-tetrahydropyridine; n.s.: not significant; NaA: sodium acetate; NaB: sodium butyrate; NaP: sodium propionate; PD: Parkinson's disease; SCFA: short-chain fatty acid; TH: tyrosine hydroxylase.

in mouse plasma compared with the MPTP group (**Figure 5E**). By contrast, IL-1β (P = 0.0014) and TNF-α (P = 0.0095) levels were significantly increased, and plasma IL-10 (P = 0.0162) levels were decreased, by acetate treatment (**Figure 5E**). There was no difference in plasma IL-6 levels among all groups (**Figure 5E**).

Next, we sought to determine whether increased inflammatory responses occurred in the CNS following acetate administration. We found that IL-1β and IL-6 levels were elevated, while IL-8, IL-10, and iNOS (not TNF-α) levels were reduced, in the SN of mice in the MPTP group compared with control mice (**Figure 5F**). Chitosan treatment downregulated IL-1β and TNF-α and upregulated IL-10 in the SN compared with the MPTP group (**Figure 5F**). Acetate supplementation elevated TNF-α expression and reduced IL-6 and IL-10 expression in the SN compared with the chitosan group (**Figure 5F**). There no significant differences in IL-1β, IL-6, or TNF-α expression levels in cerebrospinal fluid among the groups (**Additional Figure 2F**). The presence of pro-inflammatory cytokines in the colon, plasma, and SN in MPTP-induced PD mice suggests that systemic inflammation includes neuroinflammation. Microglia are the primary resident innate immune cells of the CNS, and activated microglia secrete pro- and anti-inflammatory cytokines that contribute to neuroinflammation (Voet et al., 2019). Immunofluorescence staining for Iba1, a marker of activated microglia, showed that there were more Iba1-positive cells in the SN in the MPTP group than in the control group, and that chitosan treatment induced a marked decrease (**Figure 5G**). Acetate amplified the number of Iba1-positive cells (**Figure 5G**). These findings suggest that, in MPTP-induced PD mice treated with chitosan, acetate supplementation inhibits the expression of tight junction proteins, thereby impairing the integrity of the intestinal barrier, increasing systemic inflammation, and ultimately triggering CNS inflammation, especially in the SN.

PPARD/AMPK signaling suppresses acetate-induced inflammation in Caco-2 cells

Given our finding that acetate causes inflammation that worsens PD, we explored the mechanisms associated with this effect by performing RNA sequencing of colons tissue. We identified 4934 differentially expressed genes (DEGs) by comparing the MPTP + chitosan group *vs*. the MPTP + chitosan + NaA group, among which 2756 genes were upregulated and 2178 were downregulated. There were 523 DEGs between the MPTP and MPTP + chitosan groups, among which 387 were upregulated and 136 were downregulated (**Figure 6A**). As shown in the Venn diagram in **Figure 6A**, there were 183 common DEGs between MPTP and MPTP + chitosan groups and between MPTP + chitosan and MPTP + chitosan + NaA groups. Kyoto Encyclopedia of Genes and Genomes pathway analysis of the common DEGs showed that they were enriched in the PPAR and AMPK signaling pathways, which are associated with inflammation (**Figure 6B**). Heatmaps of the DEGs are presented in **Figure 6C**. Expression changes in the DEGs within the PPAR (SCD1, SCD4, PPARD, FABP5) and AMPK (fatty acid synthase (FASN)) signaling pathways were confirmed by QPCR. Compared with the MPTP group, chitosan treatment significantly decreased SCD4 (P = 0.0379) and increased SCD1 (P = 0.0233), PPARD (P = 0.0436), and FABP5 (P = 0.0330) mRNA levels in the colon, while there was no significant difference in FASN mRNA levels between these two groups. Acetate supplementation significantly reduced the relative mRNA levels of SCD1 (P = 0.0283), PPARD (P = 0.0083), and FABP5 (P = 0.0276), while SCD4 and FASN relative mRNA levels showed no significant differences (**Figure 6D**). These results suggest that the PPAR or AMPK pathway may mediate chitosan regulation of inflammation to relieve PD symptoms via acetate reduction.

We next sought to identify the pathways that participate in acetate-mediated inflammatory responses. Studies have reported that the PPAR and AMPK signaling pathways regulate inflammation and each other (Chaturvedi and Beal, 2008; Curry et al., 2018). To explore the effects of PPARD and AMPK signaling, we employed the PPARD agonist GW0742 in enterocyte-like Caco-2 cells, which has been used extensively as a specialized model of intestinal epithelial cells *in vitro* (Alrefai et al., 2007). Cells treated with GW0742 showed an increasing trend in PPARD expression relative to untreated cells. However, the PPARD levels in the NaA group were lower than those in the control group and the NaA + GW0742 group (**Figure 7A**). To test whether the PPARD agonist regulates AMPK activity, we measured changes in AMPK and phosphorylation AMPK (p-AMPK) in cells treated with GW0742. Compared with the control group, the group treated with GW0742 exhibited significantly elevated p-AMPK (but not AMPK) levels, while treatment with acetate alone reduced p-AMPK but not AMPK protein levels (P = 0.0491). In addition, p-AMPK levels were higher in the group treated with acetate and the PPARD agonist compared with the acetate-only group (**Figure 7B**).

Acetate-treated Caco-2 cells exhibited higher levels of IL-1β, IL-6, TNF-α, and iNOS, and lower levels of IL-8, expression than control cells (**Figure 7C**). Treatment with the PPARD agonist decreased IL-1β, IL-6, IL-8, IL-10, and TNF-α expression and enhanced iNOS expression compared with the control group (**Figure 7C**). Compared with the acetate group, IL-1β (P = 0.0004) and TNF-α (P < 0.0001) expression levels were significantly downregulated, but IL-6, IL-8, and IL-10 expression levels showed no significant difference, in cells treated with acetate and the PPARD agonist (**Figure 7C**). These data suggest that treatment with the PPARD agonist promotes AMPK phosphorylation and inhibits inflammation in Caco-2 cells.

AMPK has potent anti-inflammatory effects in several cell types (Salt and Palmer, 2012); however, whether AMPK is required for acetate-induced inflammation is unknown. To test this, we treated Caco-2 cells with an AMPK agonist (AICAR) and found that AMPK expression levels remained stable, while p-AMPK expression increased (**Figure 7D**). The Caco-2 cells treated with acetate exhibited lower p-AMPK levels than the control group, whereas treatment with AICAR significantly increased p-AMPK expression (**Figure 7D**). Strikingly, p-AMPK levels were significantly higher in the NaA + AMPK agonist group than in cells treated with NaA alone (P = 0.0353; **Figure 7D**). Treatment with the AMPK agonist did not alter PPARD expression (**Figure 7E**). Next we asked whether treating Caco-2 cells with the AMPK agonist would reduce inflammation. Compared with the control group, acetate supplementation significantly increased IL-1β (P < 0.0001), IL-6 (P < 0.0001), iNOS (P = 0.0045) and TNF-α (P < 0.0001) mRNA levels and decreased IL-8 mRNA levels (P = 0.0032; **Figure 7F**). Treatment with the AMPK agonist markedly reduced IL-1β (P < 0.0001), iNOS (P = 0.0086), TNF-α (P = 0.0044), and IL-6 mRNA levels compared with the NaA group (P < 0.0001; **Figure 7F**). Cells treated with both acetate and the AMPK agonist exhibited lower IL-1β, IL-6, TNF-α, and iNOS expression levels than cells treated with acetate alone; however, no differences were observed in IL-8 and IL-10 expression between these two groups (**Figure 7F**). These findings suggest that acetate attenuates PPARD and AMPK pathway activation, thereby exacerbating inflammation in Caco-2 cells.

Chitosan reduces acetate, thereby suppress inflammation, through the PPARD/AMPK signaling pathway in an MPTP-induced mouse model of Parkinson's disease

Next, we tested whether PPARD and AMPK signaling are involved in the chitosan-mediated inhibition of inflammation via acetate in the MPTP-induced mouse model of PD. p-AMPK and PPARD expression levels in the colon of MPTP-induced PD mice were decreased compared with the control group, and treatment with chitosan eliminated this effect (**Figure 8A** and **B**). Supplementation with acetate partially restored p-AMPK and PPARD expression levels (**Figure 8A** and **B**). Consistent with the results shown in **Figure 7**, there was no significant difference in AMPK expression among the four groups (**Figure 8A** and **B**). To determine whether chitosan inhibits PPARD or AMPK expression in the SN via acetate, we examined PPARD, p-AMPK, and AMPK expression in the SN. However, no significant differences were observed in the expression levels of these proteins among the control, MPTP, MPTP + chitosan, and MPTP + chitosan + NaA groups (**Additional Figure 3A** and **B**).

A previous study has shown that PPARD activation has anti-inflammatory effects in neuroinflammation-related diseases (Bishop-Bailey and Bystrom, 2009). Therefore, we asked whether the PPARD antagonist GSK0660 could alleviate the neuroprotective effects of chitosan in the MPTP-induced mouse model of PD. As shown in **Figure 8C**, mouse body weight decreased significantly following treatment with the PPARD antagonist (P = 0.0010). Next, we examined the effect of the PPARD antagonist on motor deficits and found that it did not significantly alter motor dysfunction (**Figure 8D**). PPARD expression levels were lower in the group treated with both chitosan and the PPARD antagonist than in the group treated with chitosan only (**Figure 8E**). In addition, western blot analysis showed that treatment with the PPARD antagonist induced a clear decrease in TH expression (**Figure 8F**).

Treatment with the PPARD antagonist was associated with a significant decrease in ZO-1 and occludin expression in mouse colon tissue (**Figure 8G**).

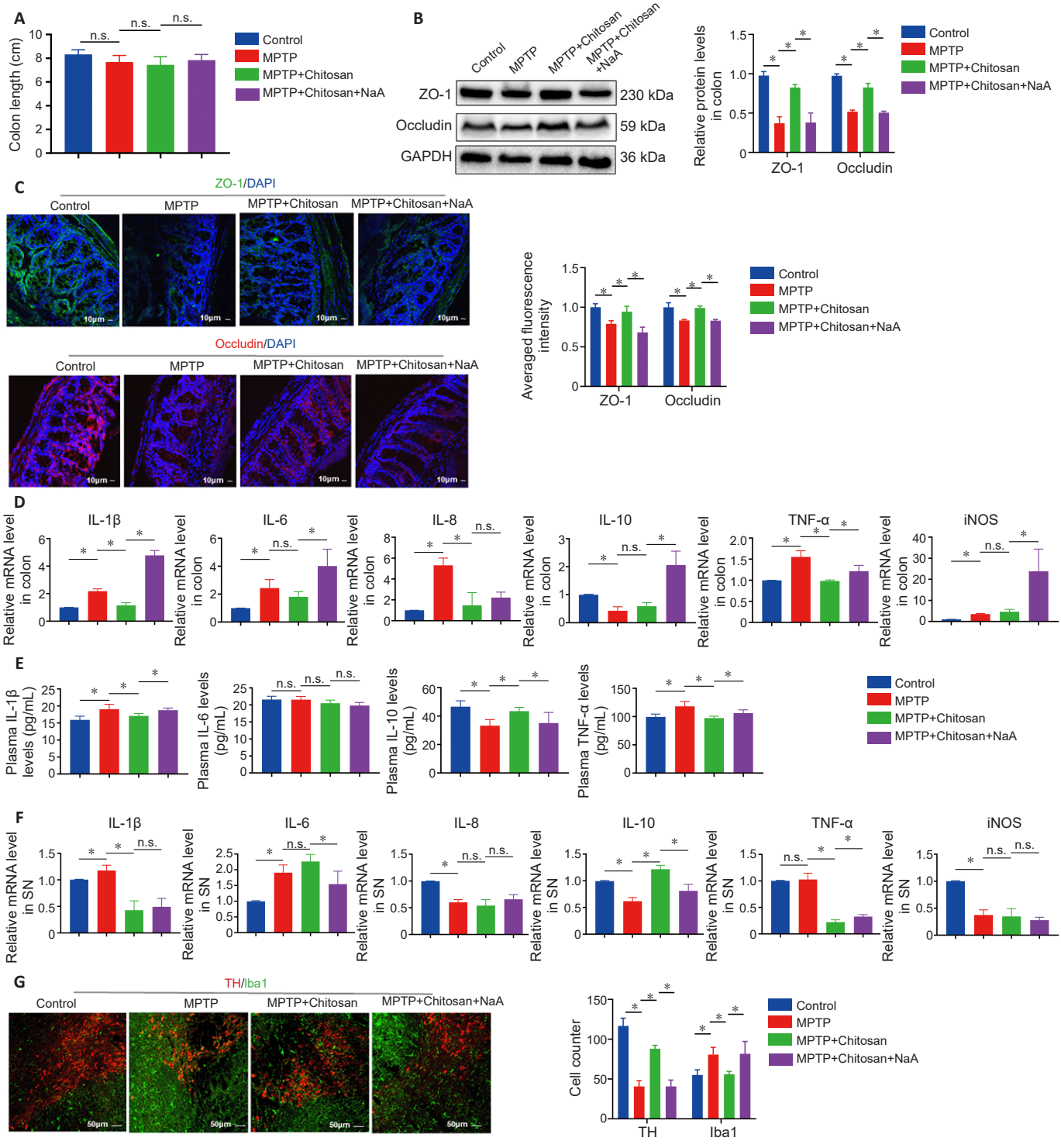

Figure 5 | **Acetate reverses chitosan-mediated repair of the intestinal barrier, increased inflammation in the colon, plasma, and SN, and promotes microglia activation in an MPTP-induced mouse model of PD.**

(A) Colon length (n = 5/group). (B) ZO-1 and occludin expression, as assessed by western blot (n = 3/group). All target proteins were normalized to the reference protein GAPDH. Compared with the chitosan group, acetate supplementation reduced ZO-1 and occludin expression levels. (C) Immunofluorescence staining for ZO-1 (green, Alexa Fluor 488) and occludin (red, Alexa Fluor 594) in mouse colon tissue (n = 3/group). The immunofluorescence results were consistent with the western blot results. Scale bars: 10 μm. (D) The relative mRNA levels of IL-1β, IL-6, IL-8, IL-10, TNF-α, and iNOS in mouse colon tissue were measured by QPCR (n = 3/group). Compared with the chitosan group, acetate supplementation resulted in an increase in IL-1β, IL-6, IL-10, TNF-α, and iNOS expression levels in the colon. The data shown in B-D were normalized to the control group. (E) The expression levels of inflammatory cytokines, including IL-1β, IL-6, IL-10, and TNF-α, in mouse plasma were measured by ELISA (n = 5/group). Compared with the chitosan group, IL-1β and TNF-α levels were significantly increased in the plasma of the acetate group, while IL-10 expression was significantly decreased. (F) The mRNA levels of IL-1β, IL-6, IL-8, IL-10, TNF-α, and iNOS (normalized to the control group) in mouse SN tissue were determined via QPCR (n = 3/group). Treatment with acetate enhanced TNF-α expression and decreased IL-6 and IL-10 expression in the SN. (G) Representative images of immunofluorescence staining for Iba1 (green, Alexa Fluor 488) and TH (red, Alexa Fluor 594) in the SN (n = 3/group). The chitosan group exhibited fewer microglia than the MPTP group, while the chitosan + acetate group exhibited more microglia than the chitosan-only group. Scale bars: 50 μm. All data are presented as the mean±SD. All experiments were repeated at least three times. *P < 0.05 (one-way analysis of variance followed by Tukey's multiple comparisons test [A–C, G] or unpaired t-test [D–F]). DAPI: 4′,6-Diamidino-2-phenylindole; ELISA: enzyme-linked immunosorbent assay; GAPDH: glyceraldehyde-3-phosphate dehydrogenase; Iba1: ionized calcium-binding adapter molecule 1; IL-1β: interleukin-1 beta; IL-6: interleukin-6; IL-8: interleukin-8; IL-10: interleukin-10; iNOS: inductible nitric oxide synthase; MPTP: 1-methyl-4-phenyl-1,2,3,6-tetrahydropyridine; n.s.: no significance; NaA: sodium acetate; PD: Parkinson's disease; QPCR: quantitative polymerase chain reaction; SN: substantia nigra; TH: tyrosine hydroxylase; TNF-α: tumor necrosis factor alpha; ZO-1: Zonula occludens-1.

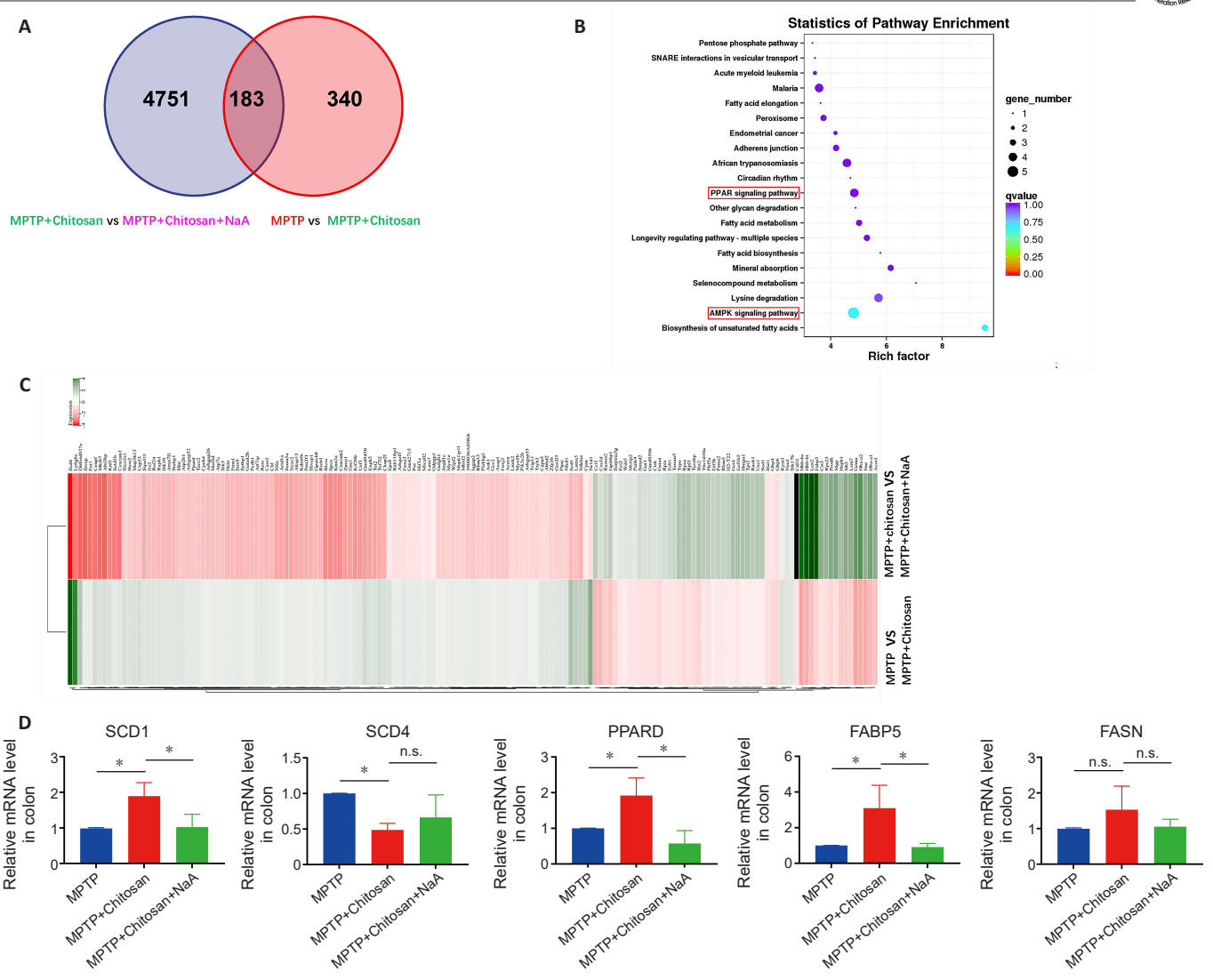

Figure 6 | **The PPAR and AMPK signaling pathways are enriched in genes whose expression is altered by acetate supplementation, as determined by RNA sequencing of colon tissue from a mouse model of PD.**

(A) Venn diagram of DEGs among three datasets. (B) KEGG pathway enrichment analysis showed that these DEGs were enriched in the PPAR and AMPK signaling pathways, which are associated with inflammation. (C) Heatmap analysis of 183 common DEGs between MPTP *vs*. MPTP + Chitosan and MPTP + Chitosan *vs*. MPTP + Chitosan + NaA (n = 2/group). (D) qPCR verification analysis of the mRNA levels (normalized to the control group) of the PPAR and AMPK signaling pathway–related genes whose expression was altered in mouse colon tissue (n = 3/group). All data are presented as the mean±SD. All experiments were repeated three times. *P < 0.05 (one-way analysis of variance followed by Tukey's multiple comparisons test). AMPK: Adenosine 5′-monophosphate-activated protein kinase; DEGs: differentially expressed genes; FABP5: fatty acid-binding protein 5; FASN: fatty acid synthase; KEGG: Kyoto Encyclopedia of Genes and Genomes; MPTP: 1-methyl-4-phenyl-1,2,3,6-tetrahydropyridine; n.s.: not significant; NaA: sodium acetate; PD: Parkinson's disease; PPAR: peroxisome proliferators-activated receptor; PPARD: peroxisome proliferator-activated receptor delta; qPCR: quantitative polymerase chain reaction; SCD1: stearoyl-coenzyme A desaturase 1; SCD4: stearoyl-coenzyme A desaturase 4.

Consistent with these results, we found that ZO-1 (P = 0.0339) and occludin (P = 0.0228) fluorescence intensities were significantly lower in the presence of the PPARD antagonist compared with the chitosan group (**Figure 8H**). IL-6 (P = 0.0443) and TNF-α (P = 0.035) mRNA levels were significantly elevated after administration of the PPARD antagonist (**Figure 8I**). Compared with mice that did not receive the PPARD antagonist, plasma IL-1β (P = 0.0014), IL-6 (P = 0.0069), and TNF-α (P < 0.0001) levels were significantly elevated in the PPARD antagonist group (**Figure 8J**). IL-1β (P = 0.0001), IL-6 (P = 0.0326), and IL-8 (P = 0.0452) levels were significantly higher in mice exposed to the PPARD antagonist than mice that were not exposed to the PPARD antagonist (**Figure 8K**). The findings suggest that the PPARD antagonist aggravates inflammation in the colon, plasma, and SN. Interestingly, p-AMPK expression in the colon was significantly reduced in mice treated with the PPARD antagonist compared with the chitosan group (P = 0.0349), but AMPK expression levels did not change (**Figure 8L**). This finding suggests that the PPARD antagonist significantly increased DA neuron death in the SN and aggravated inflammation in the colon, plasma, and SN in an MPTP-induced mouse model of PD. Taken together, our data suggest that PPARD/AMPK signaling suppresses neuroinflammation caused by chitosan reducing acetate in PD.

Discussion

The role of SCFAs in nervous system diseases such as PD, Alzheimer's disease, and autism spectrum disorder has received extensive attention; however, their effects remain incompletely understood. Numerous studies have suggested that SCFAs had a negative effect on PD. An SCFA mixture significantly activates microglia cells, accelerated α-syn aggregation, and aggravated motor dysfunction (Sampson et al., 2016). One study found that increased SCFA levels are detrimental in an MPTP-induced mouse model of PD, and that reducing SCFA levels suppresses TLR4/TNF-α signaling in the gut and brain, ultimately inhibiting neuroinflammation and relieving PD symptoms (Sun et al., 2018). Another study showed that sodium butyrate damages the intestinal barrier, triggers systemic inflammation, activates microglia and astrocytes in the striatum, promotes the secretion of inflammatory cytokines, and accelerates the death of DA neurons *in vivo*, while *in vitro* it induced inflammation by promoting secretion of the pro-inflammatory cytokines IL-1β and IL-18 from microglia (Qiao et al., 2020). Nevertheless, other studies have reported contradictory results. Hou et al. (2021) found that butyrate inhibits NF-κB and MAPK signaling, thereby decreasing neuroinflammation and alleviate symptoms of PD, while high-dose sodium acetate increases DA

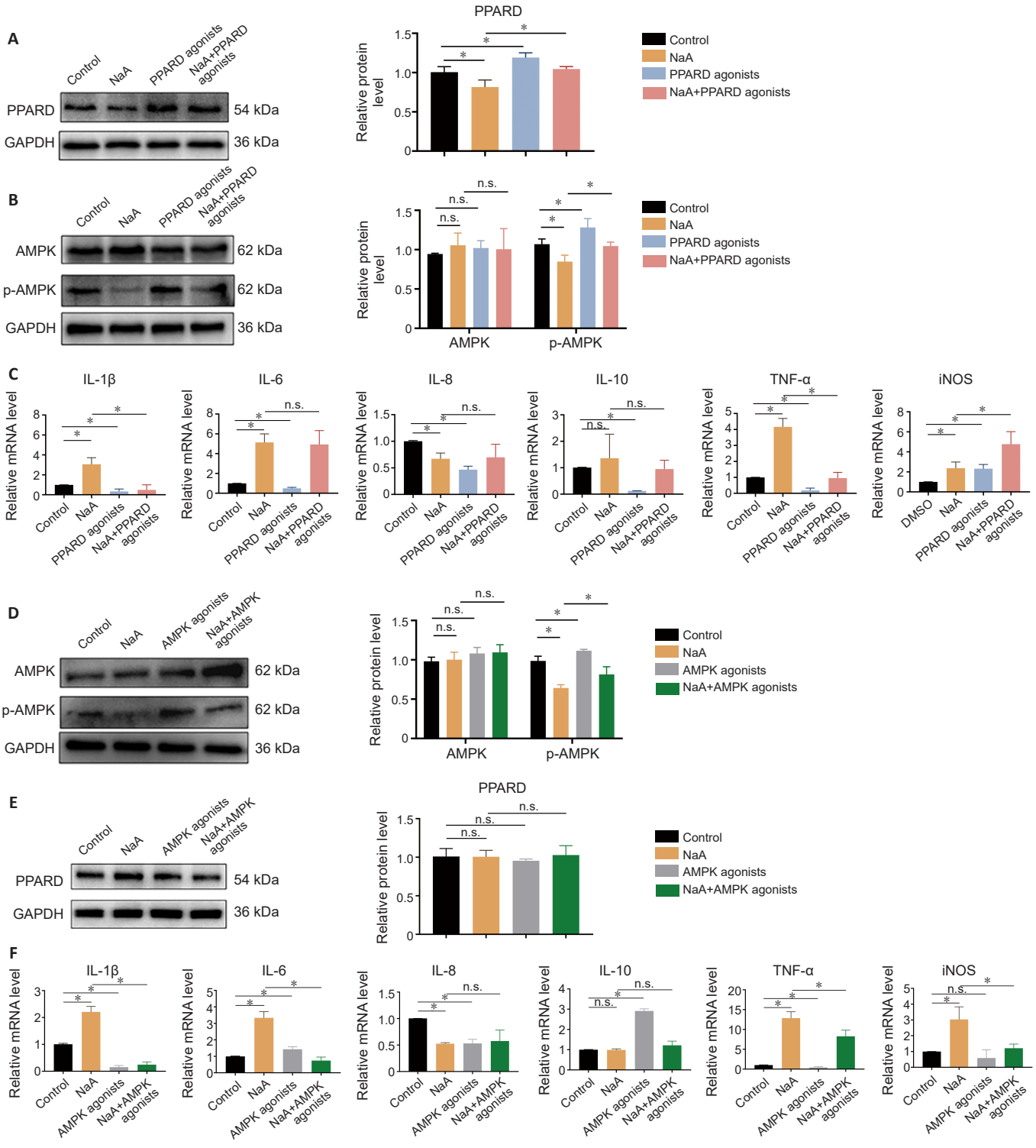

Figure 7 | **Acetate may relieve inflammation by activating the PPARD/AMPK signaling pathway in Caco-2 cells.**

(A, B) Western blot analysis of PPARD, p-AMPK, and AMPK expression in Caco-2 cells treated with a PPARD agonist or left untreated. Compared with the acetate group, PPARD and p-AMPK expression levels were significantly increased in the group treated with acetate and the PPARD agonist. (C) qPCR was used to detect the mRNA level of IL-1β, IL-6, IL-8, IL-10, TNF-α, and iNOS in Caco-2 cells treated with a PPARD agonist or left untreated. Compared with the acetate group, IL-1β and TNF-α were down-regulated, and iNOS was up-regulated, in cells treated with the PPARD agonist. (D, E) Western blot analysis of AMPK, p-AMPK, and PPARD expression levels in Caco-2 cells treated with an AMPK agonist or left untreated. p-AMPK expression was significantly lower in the group treated with acetate and an AMPK agonist than in the acetate-only group. PPARD expression was not altered by treatment with the AMPK agonist. (F) qPCR was used to detect the mRNA levels of IL-1β, IL-6, IL-8, IL-10, TNF-α, and iNOS in Caco-2 cells treated with the AMPK agonist or left untreated. Treatment with the AMPK agonist reduced IL-1β, iNOS, IL-6, and TNF-α expression levels compared with treatment with acetate alone. GAPDH was used as loading control in the western blot assays. All data (normalized by control group) are presented as the mean ± SD (n = 3/group). All experiments were repeated at least three times. *P < 0.05 (one-way analysis of variance followed by Tukey's multiple comparisons test). AMPK: Adenosine 5′-monophosphate-activated protein kinase; GAPDH: glyceraldehyde-3-phosphate dehydrogenase; IL-1β: interleukin-1 beta; IL-6: interleukin-6; IL-8: interleukin-8; IL-10: interleukin-10; iNOS: inductible nitric oxide synthase; n.s.: no significance; p-AMPK: phosphorylation adenosine 5′-monophosphate-activated protein kinase; PPARD: peroxisome proliferator-activated receptor delta; qPCR: quantitative polymerase chain reaction; TNF-α: tumor necrosis factor alpha.

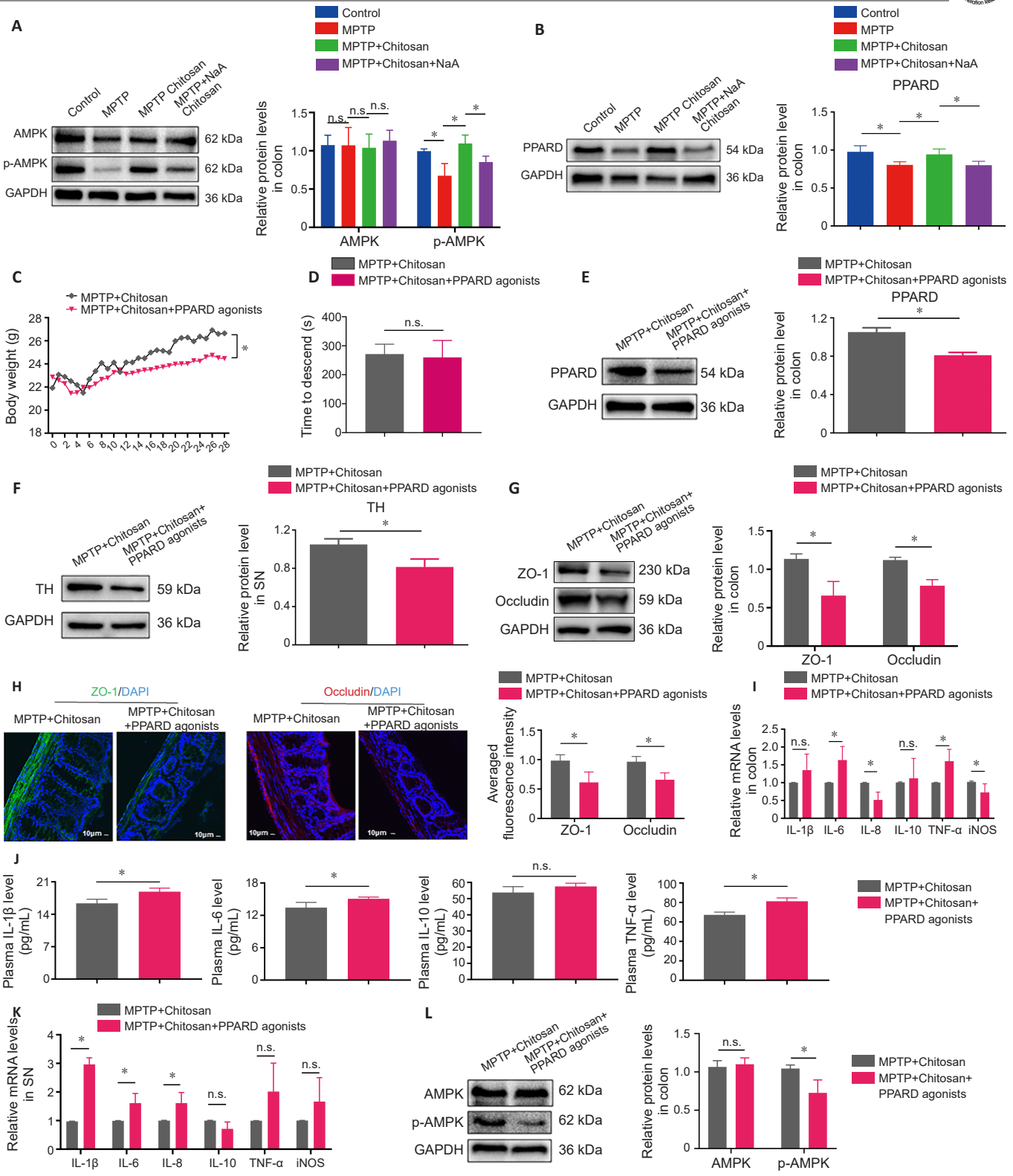

Figure 8 | **Chitosan may reduce acetate levels, thereby activating the PPARD-AMPK signaling pathway, which promotes repair of the intestinal barrier and reduces neuroinflammation in an MPTP-induced mouse model of PD.**

(A, B) Western blot analysis of p-AMPK, AMPK, and PPARD levels in mouse colon tissue (n = 3/group). Treatment with acetate significantly increased p-AMPK and PPARD expression. (C) Treatment with a PPARD antagonist significantly decreased mouse body weight (n = 6/group). (D) There were no significant differences in fall latency among the groups in the rotarod test, which was used to assess motor dysfunction (n = 6/group). (E–G) PPARD antagonist treatment significantly decreased PPARD, TH, ZO-1, and occludin expression, as determined by western blot (n = 3/group). (H) Immunofluorescence staining for ZO-1 (green, Alexa Fluor 488) and occludin (red, Alexa Fluor 594) in mouse colon tissue (n = 3/group). The PPARD antagonist treatment group exhibited markedly reduced ZO-1 and occludin mRNA expression levels in colon tissue. Scale bars: 10 μm. (I) QPCR was used to measure the mRNA levels of IL-1β, IL-6, IL-8, IL-10, TNF-α, and iNOS in mouse colon tissue (n = 3/group). Treatment with the PPARD antagonist increased IL-6 and TNF-α mRNA levels, while IL-8 and iNOS levels were reduced. (J) ELISA was used to detect IL-1β, IL-6, IL-10, and TNF-α expression levels in mouse plasma (n = 5/group). IL-1β, IL-6, and TNF-α expression levels were significantly increased in the PPARD antagonist treatment group. (K) QPCR was used to measure mRNA levels of IL-1β, IL-6, IL-8, IL-10, TNF-α, and iNOS in the SN (n = 3/group). Treatment with the PPARD antagonist significantly increased the mRNA levels of IL-1β, IL-6, and IL-8. (L) Treatment with the PPARD antagonist reduced p-AMPK, but not AMPK, expression (n = 3/group). GAPDH was used as the internal reference. All data are presented as the mean ± SD. All experiments were repeated at least three times. *P < 0.05 (one-way analysis of variance followed by Tukey's multiple comparisons test (A, B) or unpaired t-test (C–L)). AMPK: Adenosine 5′-monophosphate-activated protein kinase; DAPI: 4′,6-diamidino-2-phenylindole; GAPDH: glyceraldehyde-3-phosphate dehydrogenase; IL-1β: interleukin-1 Beta; IL-6: interleukin-6; IL-8: interleukin-8; IL-10: interleukin-10; iNOS: inductible nitric oxide synthase; n.s.: not significant; NaA: sodium acetate; p-AMPK: phosphorylation adenosine 5′-monophosphate-activated protein kinase; PD: Parkinson's disease; PPARD: peroxisome proliferator-activated receptor delta; QPCR: quantitative polymerase chain reaction; SN: substantia nigra; TH: tyrosine hydroxylase; TNF-α: tumor necrosis factor alpha; ZO-1: Zonula occludens-1.

neuron numbers and reduces α-syn accumulation in PD mice. In addition, clinical studies have shown that fecal and plasma acetate, propionate, and butyrate levels differ significantly between patients with PD and healthy controls, and that SCFA levels correlated with the PD severity (Shin et al., 2020; Toczylowska et al., 2020; Chen et al., 2022). Hence, the effect and mechanism of SCFAs are as yet undefined. The conflicting reports about the effects of SCFAs, even in the same models, are likely because of the absence of integrated and systematic assessment of feces, plasma, and brain SCFA levels in PD models. Our study found that the feces of MPTP-induced PD model mice contained more sodium acetate than the feces of control mice, and that chitosan treatment reduced fecal sodium acetate levels, which correlated with a reduction in DA neuron injury. Acetate supplementation after chitosan treatment increased motor dysfunction, elevated inflammatory cytokine levels in the colon, peripheral blood, and SN, increased the death rate of DA neurons, and exacerbated PD symptoms. Moreover, there was no significant difference in SCFA levels in the plasma or brain between the PD and chitosan treatment groups. Therefore, we believe that SCFAs in the gut trigger neuroinflammation in this mouse model of PD.

SCFAs modulate microbiome–gut–brain communication primarily through immune, endocrine, vagal, and other humoral pathways (Dalile et al., 2019). In the immune pathway, SCFAs affect intestinal mucosal immunity and barrier function to regulate systemic inflammation. The GBB acts as a physiological barrier that plays a pivotal role in protecting the peripheral system against attacks from toxins and pathogens. Recent studies have shown that SCFAs are associated with GBB permeability. At physiological concentrations, SCFAs may ensure GBB integrity, thereby decreasing the permeability of colonic epithelium. Butyrate promotes tight junction protein expression, reducing intestinal permeability (Ma et al., 2012; Zheng et al., 2017; Feng et al., 2018). Likewise, acetate protects intestinal barrier integrity by promoting Caco-2 cell survival in the presence of pathogens. Another study showed that acetate produced by Heligmosomoides polygyrus reduces the expression of epithelial tight junction proteins and damages the gut barrier, allowing the pathogen to establish chronic infections (Schälter et al., 2022). Recent clinical data demonstrated that patients with PD have decreased SCFA concentrations, increased GBB permeability, and an elevated ratio of plasma/fecal SCFAs than healthy subjects (Yang et al., 2022). In our study we found that MPTP-induced PD model mice had high GBB permeability, and that treatment with chitosan reduced acetate levels, suppressed the expression of pro-inflammatory factors, and restored GBB integrity.

SCFAs can promote BBB tight junction proteins, thereby increasing BBB integrity, via G protein–coupled receptors (Braniste et al., 2014; Blacher et al., 2017; Dalile et al., 2019). Acetate and propionate produced by *Clostridium tyrobutyricum* enhance the expression of tight junction proteins and improve BBB barrier function but do not change large vascular structures in germ-free mice that lack a normal gut microbiota and have poor BBB integrity (Braniste et al., 2014). After traumatic brain injury, butyrate supplementation decreases neuronal damage by increasing occludin and ZO-1 expression and maintaining BBB integrity. PD mice treated with polymannuronic acid display increased fecal SCFA content, reduced inflammation, restored GBB and BBB integrity manifesting as enhanced expression of tight junction proteins, and finally, symptom remission (Dong et al., 2020). Nonetheless, it remained unclear whether SCFAs affect the BBB in PD. In the present study, we found that the BBB was damaged in an MPTP-induced mouse model of PD, and that a reduction in acetate levels in the intestine induced by chitosan treatment suppressed the expression of pro-inflammatory factors and restored BBB integrity without changing SCFA levels in the plasma or the brain; however, supplementation with acetate increased inflammation, impaired the GBB, and aggravated PD symptoms. SCFAs can cross the BBB to maintain CNS integrity and function. However, brain SCFA levels were comparable in the chitosan treatment group and the MPTP-induced PD group, suggesting that BBB permeability may be regulated by intestinal inflammation, not SCFAs. In addition, while GBB integrity was disrupted, plasma SCFA levels remained unchanged. To our knowledge, this is the first study to simultaneously measure SCFA concentrations in feces, plasma, and brains in an MPTP-induced mouse model of PD.

There were some limitations to this study. First, while we analyzed microbial metabolites, we did not confirm the role of gut microbes in this study. Second, while there are many types of microbial metabolites, we focused on the SCFAs. Thus, chitosan may regulate other microbial metabolites to exert its effects on PD symptoms. Finally, the potential effects of chitosan on reducing SCFA levels or regulating the balance of SCFAs deserve further study.

In conclusion, our study shows that chitosan reduced gut flora diversity and SCFA levels (especially acetate), inhibited PPARD/AMPK signaling and relieved inflammation in the colon, plasma, and SN, and repaired the damaged GBB and BBB, thereby alleviating PD symptoms. These findings suggest that chitosan should be used to prevent and manage PD by decreasing SCFA levels.

Acknowledgments: *We sincerely thank Chen Shen (The Central Laboratory of the Second Affiliated Hospital, Kunming Medical University) for drawing the schematic model.*
Author contributions: *Study design, supervision and manuscript review: JY, NZ and ZY; experiment performance, data collection and manuscript draft: YW and RC; behavioral data collection: GS; data analysis and figure preparation: KL and RW; manuscript revision and experimental support: XH and XC. All authors read and approved the final version of the manuscript.*
Conflicts of interest: *There are no conflicts of interest.*
Data availability statement: *All relevant data are within the paper and its Additional files.*
Open access statement: *This is an open access journal, and articles are distributed under the terms of the Creative Commons Attribution-NonCommercial-ShareAlike 4.0 License, which allows others to remix, tweak, and build upon the work non-commercially, as long as appropriate credit is given and the new creations are licensed under the identical terms.*
Open peer reviewer: *Jyoti Ahlawat, The University of Texas, USA.*
Additional files:
Additional Figure 1: *Chitosan administration is unable to change intestinal fungi in MPTP-induced PD mice using ITS sequencing.*
Additional Figure 2: *Acetate alone has no effect on TH positive neurons or inflammation, and chitosan does not regulate inflammatory response in cerebrospinal fluid.*
Additional Figure 3: *The protein expression levels of PPARD and p-AMPK are unchanged in the substantia nigra with different treatment.*

References

Ahmadi S, Mainali R, Nagpal R, Sheikh-Zeinoddin M, Soleimanian-Zad S, Wang S, Deep G, Kumar Mishra S, Yadav H (2017) Dietary polysaccharides in the amelioration of gut microbiome dysbiosis and metabolic diseases. Obes Control Ther 4:10.15226/2374-8354/4/2/00140.

Alarcón TA, Presti-Silva SM, Simões APT, Ribeiro FM, Pires RGW (2023) Molecular mechanisms underlying the neuroprotection of environmental enrichment in Parkinson's disease. Neural Regen Res 18:1450-1456.

Alrefai WA, Saksena S, Tyagi S, Gill RK, Ramaswamy K, Dudeja PK (2007) Taurodeoxycholate modulates apical Cl-/OH- exchange activity in Caco2 cells. Dig Dis Sci 52:1270-1278.

Baxter MFA, Merino-Guzman R, Latorre JD, Mahaffey BD, Yang Y, Teague KD, Graham LE, Wolfenden AD, Hernandez-Velasco X, Bielke LR, Hargis BM, Tellez G (2017) Optimizing fluorescein isothiocyanate dextran measurement as a biomarker in a 24-h feed restriction model to induce gut permeability in broiler chickens. Front Vet Sci 4:56.

Bhattamisra SK, Shak AT, Xi LW, Safian NH, Choudhury H, Lim WM, Shahzad N, Alhakamy NA, Anwer MK, Radhakrishnan AK, Md S (2020) Nose to brain delivery of rotigotine loaded chitosan nanoparticles in human SH-SY5Y neuroblastoma cells and animal model of Parkinson's disease. Int J Pharm 579:119148.

Bishop-Bailey D, Bystrom J (2009) Emerging roles of peroxisome proliferator-activated receptor-beta/delta in inflammation. Pharmacol Ther 124:141-150.

Blacher E, Levy M, Tatirovsky E, Elinav E (2017) Microbiome-modulated metabolites at the interface of host immunity. J Immunol 198:572-580.

Braniste V, Al-Asmakh M, Kowal C, Anuar F, Abbaspour A, Tóth M, Korecka A, Bakocevic N, Ng LG, Kundu P, Gulyás B, Halldin C, Hultenby K, Nilsson H, Hebert H, Volpe BT, Diamond B, Pettersson S (2014) The gut microbiota influences blood-brain barrier permeability in mice. Sci Transl Med 6:263ra158.

Brown HE, Esher SK, Alspaugh JA (2020) Chitin: a "hidden figure" in the fungal cell wall. Curr Top Microbiol Immunol 425:83-111.

Chaturvedi RK, Beal MF (2008) PPAR: a therapeutic target in Parkinson's disease. J Neurochem 106:506-518.

Chen QQ, Liu QY, Wang P, Qian TM, Wang XH, Yi S, Li SY (2023) Potential application of let-7a antagomir in injured peripheral nerve regeneration. Neural Regen Res 18:1584-1590.

Chen SJ, Chen CC, Liao HY, Lin YT, Wu YW, Liou JM, Wu MS, Kuo CH, Lin CH (2022) Association of fecal and plasma levels of short-chain fatty acids with gut microbiota and clinical severity in patients with Parkinson disease. Neurology 98:e848-e858.

Curry DW, Stutz B, Andrews ZB, Elsworth JD (2018) Targeting AMPK signaling as a neuroprotective strategy in Parkinson's disease. J Parkinsons Dis 8:161-181.

Dalile B, Van Oudenhove L, Vervliet B, Verbeke K (2019) The role of short-chain fatty acids in microbiota-gut-brain communication. Nat Rev Gastroenterol Hepatol 16:461-478.

Do J, Foster D, Renier C, Vogel H, Rosenblum S, Doyle TC, Tse V, Wapnir I (2014) Ex vivo Evans blue assessment of the blood brain barrier in three breast cancer brain metastasis models. Breast Cancer Res Treat 144:93-101.

Dong XL, Wang X, Liu F, Liu X, Du ZR, Li RW, Xue CH, Wong KH, Wong WT, Zhao Q, Tang QJ (2020) Polymannuronic acid prevents dopaminergic neuronal loss via brain-gut-microbiota axis in Parkinson's disease model. Int J Biol Macromol 164:994-1005.

El Kaoutari A, Armougom F, Gordon JI, Raoult D, Henrissat B (2013) The abundance and variety of carbohydrate-active enzymes in the human gut microbiota. Nat Rev Microbiol 11:497-504.

Feng W, Wu Y, Chen G, Fu S, Li B, Huang B, Wang D, Wang W, Liu J (2018) Sodium butyrate attenuates diarrhea in weaned piglets and promotes tight junction protein expression in colon in a GPR109A-dependent manner. Cell Physiol Biochem 47:1617-1629.

Gallaher CM, Munion J, Hesslink R, Jr., Wise J, Gallaher DD (2000) Cholesterol reduction by glucomannan and chitosan is mediated by changes in cholesterol absorption and bile acid and fat excretion in rats. J Nutr 130:2753-2759.

Hou Y, Li X, Liu C, Zhang M, Zhang X, Ge S, Zhao L (2021) Neuroprotective effects of short-chain fatty acids in MPTP induced mice model of Parkinson's disease. Exp Gerontol 150:111376.

Jackson-Lewis V, Przedborski S (2007) Protocol for the MPTP mouse model of Parkinson's disease. Nat Protoc 2:141-151.

Jaworska K, Konop M, Bielinska K, Hutsch T, Dziekiewicz M, Banaszkiewicz A, Ufnal M (2019) Inflammatory bowel disease is associated with increased gut-to-blood penetration of short-chain fatty acids: A new, non-invasive marker of a functional intestinal lesion. Exp Physiol 104:1226-1236.

Kumar H, Kim IS, More SV, Kim BW, Bahk YY, Choi DK (2013) Gastrodin protects apoptotic dopaminergic neurons in a toxin-induced Parkinson's disease model. Evid Based Complement Alternat Med 2013:514095.

Laferriere CA, Pang DS (2020) Review of intraperitoneal injection of sodium pentobarbital as a method of euthanasia in laboratory rodents. J Am Assoc Lab Anim Sci 59:254-263.

Lima IS, Pêgo AC, Martins AC, Prada AR, Barros JT, Martins G, Gozzelino R (2023) Gut dysbiosis: a target for protective interventions against Parkinson's disease. Microorganisms 11:880.

Liu XY, Wei MG, Liang J, Xu HH, Wang JJ, Wang J, Yang XP, Lv FF, Wang KQ, Duan JH, Tu Y, Zhang S, Chen C, Li XH (2020) Injury-preconditioning secretome of umbilical cord mesenchymal stem cells amplified the neurogenesis and cognitive recovery after severe traumatic brain injury in rats. J Neurochem 153:230-251.

Liu XY, Feng YH, Feng QB, Zhang JY, Zhong L, Liu P, Wang S, Huang YR, Chen XY, Zhou LX (2023) Low-temperature 3D-printed collagen/chitosan scaffolds loaded with exosomes derived from neural stem cells pretreated with insulin growth factor-1 enhance neural regeneration after traumatic brain injury. Neural Regen Res 18:1990-1998.

Livak KJ, Schmittgen TD (2001) Analysis of relative gene expression data using real-time quantitative PCR and the 2(-Delta Delta C(T)) method. Methods 25:402-408.

Ma X, Fan PX, Li LS, Qiao SY, Zhang GL, Li DF (2012) Butyrate promotes the recovering of intestinal wound healing through its positive effect on the tight junctions. J Anim Sci 90 Suppl 4:266-268.

Manigandan V, Nataraj J, Karthik R, Manivasagam T, Saravanan R, Thenmozhi AJ, Essa MM, Guillemin GJ (2019) Low molecular weight sulfated chitosan: neuroprotective effect on rotenone-induced in vitro Parkinson's disease. Neurotox Res 35:505-515.

Mendes NF, Pansani AP, Carmanhães ERF, Tange P, Meireles JV, Ochikubo M, Chagas JR, da Silva AV, Monteiro de Castro G, Le Sueur-Maluf L (2019) The blood-brain barrier breakdown during acute phase of the pilocarpine model of epilepsy is dynamic and time-dependent. Front Neurol 10:382.

Nehal N, Nabi B, Rehman S, Pathak A, Iqubal A, Khan SA, Yar MS, Parvez S, Baboota S, Ali J (2021) Chitosan coated synergistically engineered nanoemulsion of Ropinirole and nigella oil in the management of Parkinson's disease: Formulation perspective and In vitro and In vivo assessment. Int J Biol Macromol 167:605-619.

Percie du Sert N, et al. (2020) The ARRIVE guidelines 2.0: updated guidelines for reporting animal research. PLoS Biol 18:e3000410.

Pifl C, Hornykiewicz O (2006) Dopamine turnover is upregulated in the caudate/putamen of asymptomatic MPTP-treated rhesus monkeys. Neurochem Int 49:519-524.

Pramod Kumar P, Harish Prashanth KV (2020) Diet with low molecular weight chitosan exerts neuromodulation in rotenone induced Drosophila model of Parkinson's disease. Food Chem Toxicol 146:111860.

Qiao CM, Sun MF, Jia XB, Li Y, Zhang BP, Zhao LP, Shi Y, Zhou ZL, Zhu YL, Cui C, Shen YQ (2020) Sodium butyrate exacerbates parkinson's disease by aggravating neuroinflammation and colonic inflammation in MPTP-induced mice model. Neurochem Res 45:2128-2142.

Rassu G, Soddu E, Cossu M, Gavini E, Giunchedi P, Dalpiaz A (2016) Particulate formulations based on chitosan for nose-to-brain delivery of drugs. A review. J Drug Deliv Sci Technol 32:77-87.

Roy S (2017) Synuclein and dopamine: the Bonnie and Clyde of Parkinson's disease. Nat Neurosci 20:1514-1515.

Salt IP, Palmer TM (2012) Exploiting the anti-inflammatory effects of AMP-activated protein kinase activation. Expert Opin Investig Drugs 21:1155-1167.

Sampson TR, Debelius JW, Thron T, Janssen S, Shastri GG, Ilhan ZE, Challis C, Schretter CE, Rocha S, Gradinaru V, Chesselet MF, Keshavarzian A, Shannon KM, Krajmalnik-Brown R, Wittung-Stafshede P, Knight R, Mazmanian SK (2016) Gut microbiota regulate motor deficits and neuroinflammation in a model of Parkinson's disease. Cell 167:1469-1480. e12.

Sardoiwala MN, Karmakar S, Choudhury SR (2021) Chitosan nanocarrier for FTY720 enhanced delivery retards Parkinson's disease via PP2A-EzH2 signaling in vitro and ex vivo. Carbohydr Polym 254:117435.

Schälter F, Frech M, Dürholz K, Lucas S, Sarter K, Lebon L, Esser-von Bieren J, Dubey LK, Voehringer D, Schett G, Harris NL, Zaiss MM (2022) Acetate, a metabolic product of Heligmosomoides polygyrus, facilitates intestinal epithelial barrier breakdown in a FFAR2-dependent manner. Int J Parasitol 52:591-601.

Schneider CA, Rasband WS, Eliceiri KW (2012) NIH Image to ImageJ: 25 years of image analysis. Nat Methods 9:671-675.

Shin C, Lim Y, Lim H, Ahn TB (2020) Plasma short-chain fatty acids in patients with Parkinson's disease. Mov Disord 35:1021-1027.

Singh Y, Trautwein C, Romani J, Salker MS, Neckel PH, Fraccaroli I, Abeditashi M, Woerner N, Admard J, Dhariwal A, Dueholm MKD, Schäfer KH, Lang F, Otzen DE, Lashuel HA, Riess O, Casadei N (2023) Overexpression of human alpha-Synuclein leads to dysregulated microbiome/metabolites with ageing in a rat model of Parkinson disease. Mol Neurodegener 18:44.

Smith PM, Howitt MR, Panikov N, Michaud M, Gallini CA, Bohlooly YM, Glickman JN, Garrett WS (2013) The microbial metabolites, short-chain fatty acids, regulate colonic Treg cell homeostasis. Science 341:569-573.

Sun MF, Zhu YL, Zhou ZL, Jia XB, Xu YD, Yang Q, Cui C, Shen YQ (2018) Neuroprotective effects of fecal microbiota transplantation on MPTP-induced Parkinson's disease mice: Gut microbiota, glial reaction and TLR4/TNF-α signaling pathway. Brain Behav Immun 70:48-60.

Talley S, Valiauga R, Anderson L, Cannon AR, Choudhry MA, Campbell EM (2021) DSS-induced inflammation in the colon drives a proinflammatory signature in the brain that is ameliorated by prophylactic treatment with the S100A9 inhibitor paquinimod. J Neuroinflammation 18:263.

Tanaka T, Kohno H, Suzuki R, Yamada Y, Sugie S, Mori H (2003) A novel inflammation-related mouse colon carcinogenesis model induced by azoxymethane and dextran sodium sulfate. Cancer Sci 94:965-973.

Toczylowska B, Zieminska E, Michałowska M, Chalimoniuk M, Fiszer U (2020) Changes in the metabolic profiles of the serum and putamen in Parkinson's disease patients- in vitro and in vivo NMR spectroscopy studies. Brain Res 1748:147118.

Uyanga VA, Ejeromedoghene O, Lambo MT, Alowakennu M, Alli YA, Ere-Richard AA, Min L, Zhao J, Wang X, Jiao H, Onagbesan OM, Lin H (2023) Chitosan and chitosan-based composites as beneficial compounds for animal health: Impact on gastrointestinal functions and biocarrier application. J Funct Foods 104:105520.

Voet S, Prinz M, van Loo G (2019) Microglia in central nervous system inflammation and multiple sclerosis pathology. Trends Mol Med 25:112-123.

Wang Q, Wang C, Xiang X, Xu H, Han G (2022a) Analysis of microbial diversity and succession during Xiaoqu Baijiu fermentation using high-throughput sequencing technology. Eng Life Sci 22:495-504.

Wang X, Miao J, Yan C, Ge R, Liang T, Liu E, Li Q (2016) Chitosan attenuates dibutyltin-induced apoptosis in PC12 cells through inhibition of the mitochondria-dependent pathway. Carbohydr Polym 151:996-1005.

Wang Y, Chen R, Yang Z, Wen Q, Cao X, Zhao N, Yan J (2022b) Protective effects of polysaccharides in neurodegenerative diseases. Front Aging Neurosci 14:917629.

Wei KC, Chu PC, Wang HY, Huang CY, Chen PY, Tsai HC, Lu YJ, Lee PY, Tseng IC, Feng LY, Hsu PW, Yen TC, Liu HL (2013) Focused ultrasound-induced blood-brain barrier opening to enhance temozolomide delivery for glioblastoma treatment: a preclinical study. PLoS One 8:e58995.

Wu Z, Nybom P, Magnusson KE (2000) Distinct effects of Vibrio cholerae haemagglutinin/protease on the structure and localization of the tight junction-associated proteins occludin and ZO-1. Cell Microbiol 2:11-17.

Xu Y, He Q, Wang M, Wang X, Gong F, Bai L, Zhang J, Wang W (2019) Quantifying blood-brain-barrier leakage using a combination of evans blue and high molecular weight FITC-Dextran. J Neurosci Methods 325:108349.

Xue Y, Wang N, Zeng Z, Huang J, Xiang Z, Guan YQ (2020) Neuroprotective effect of chitosan nanoparticle gene delivery system grafted with acteoside (ACT) in Parkinson's disease models. J Mater Sci Technol 43:197-207.

Yang X, Ai P, He X, Mo C, Zhang Y, Xu S, Lai Y, Qian Y, Xiao Q (2022) Parkinson's disease is associated with impaired gut-blood barrier for short-chain fatty acids. Mov Disord 37:1634-1643.

Yao HT, Chiang MT (2006) Chitosan shifts the fermentation site toward the distal colon and increases the fecal short-chain fatty acids concentrations in rats. Int J Vitam Nutr Res 76:57-64.

Yao J, Wang J, Wu L, Lu H, Wang Z, Yu P, Xiao H, Gao R, Yu J (2020) Perinatal exposure to bisphenol A causes a disturbance of neurotransmitter metabolic pathways in female mouse offspring: A focus on the tryptophan and dopamine pathways. Chemosphere 254:126715.

Yu S, Xu X, Feng J, Liu M, Hu K (2019) Chitosan and chitosan coating nanoparticles for the treatment of brain disease. Int J Pharm 560:282-293.

Zheng L, Kelly CJ, Battista KD, Schaefer R, Lanis JM, Alexeev EE, Wang RX, Onyiah JC, Kominsky DJ, Colgan SP (2017) Microbial-derived butyrate promotes epithelial barrier function through IL-10 receptor-dependent repression of claudin-2. J Immunol 199:2976-2984.

P-Reviewer: Ahlawat J; C-Editor: Zhao M; S-Editors: Yu J, Li CH; L-Editors: Crow E, Yu J, Song LP; T-Editor: Jia Y

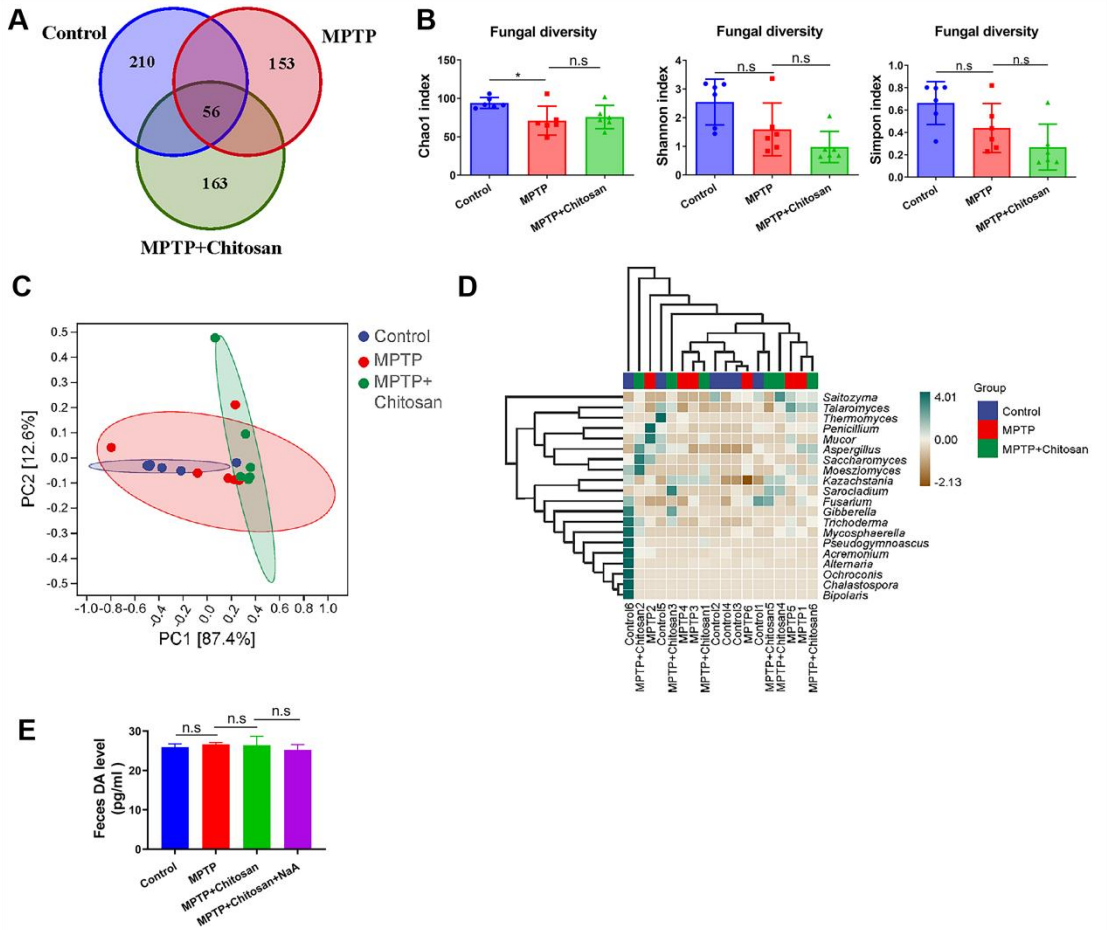

Additional Figure 1 Chitosan administration is unable to change intestinal fungi in MPTP-induced PD mice using ITS sequencing.

(A) Venn diagram of the numbers of unique and shared OTU in intestinal fungi of control, MPTP and MPTP + chitosan groups. (B) α-Diversity including Chao1 index, Shannon index, Simpon index was no change in the abundance and composition of intestinal fungi in MPTP-induced PD mice treated with chitosan. (C) β-Diversity was presented as the principal coordinate analysis plot, and there was no difference. (D) The heat map of the 20 most differentially abundant taxons among the three groups at the genus level. (E) The level of DA in mice feces was detected via ELISA. All data are presented as the mean ± SD (n = 6/group). *$P < 0.05$ (one-way analysis of variance followed by Tukey's multiple comparisons test). DA: Dopamine; ELISA: enzyme-linked immunosorbent assay; MPTP: 1-methyl-4-phenyl-1,2,3,6-tetrahydropyridine; OTU: operational taxonomic unit; PD: Parkinson's disease.

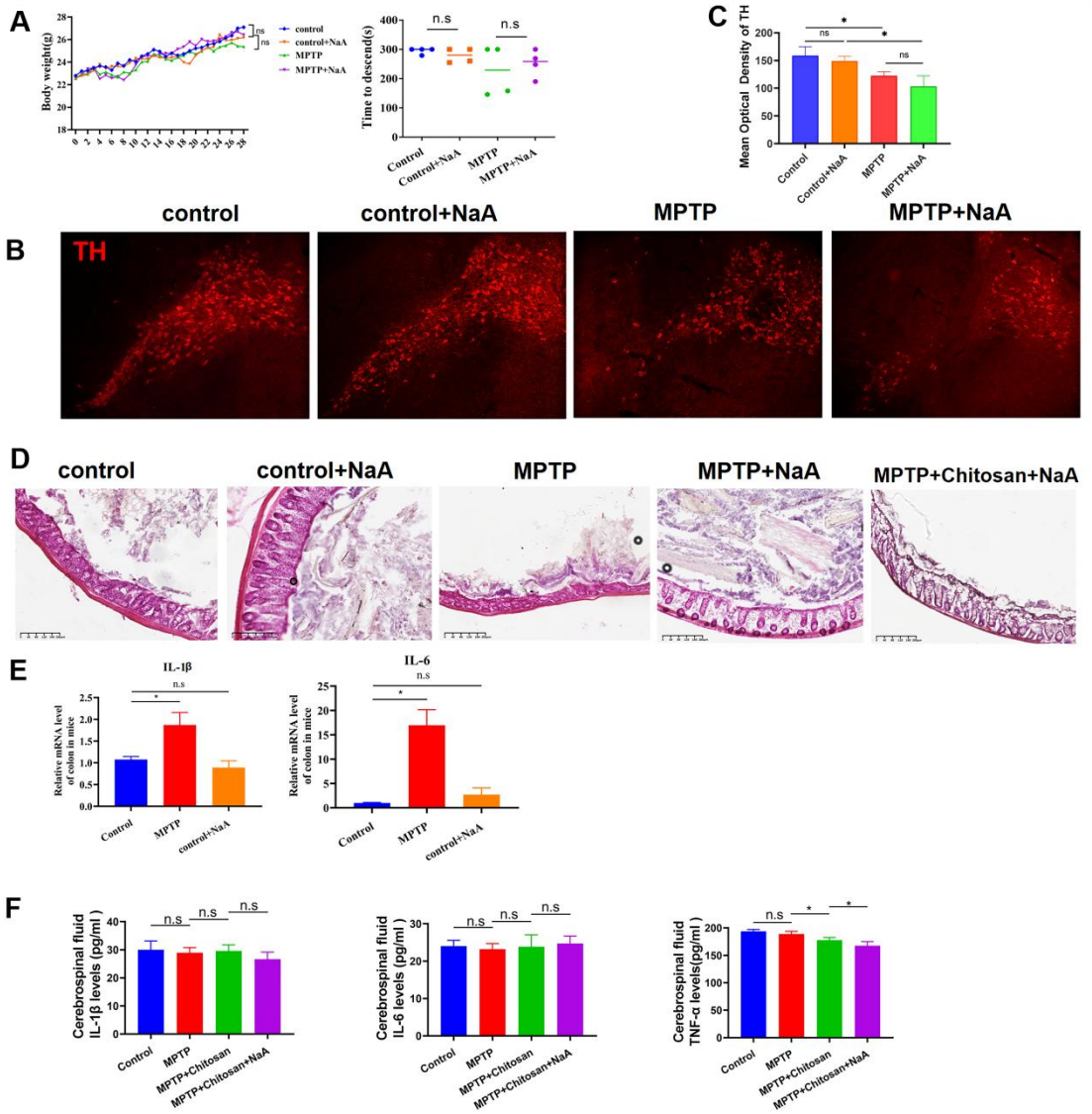

Additional Figure 2 Acetate alone has no effect on TH positive neurons or inflammation, and chitosan does not regulate inflammatory response in cerebrospinal fluid.

(A) The body weight and rotarod test of control, control + NaA, MPTP, and MPTP + NaA mice (n = 4/group). (B, C) The TH immunofluorescence staining and the quantitative analysis in control, control + NaA, MPTP, and MPTP + NaA (n = 3/group). The number of TH^+ neurons had no difference in control with or without acetate, but that of MPTP + NaA group had a reduced trend relative to MPTP group. Scale bars: 100 μm. (D) The hematoxylin-eosin staining analysis in the colon of control, control + NaA, MPTP, MPTP + NaA and MPTP + chitosan + NaA groups (n = 3/group). (E) The relative mRNA levels (normalized by control group) of inflammatory factors (IL-1β and IL-6) were tested by QPCR (n = 3/group), and the RNA was recovered from the frozen section tissue. (F) ELISA detected the level of IL-1β, IL-6 and TNF-α in cerebrospinal fluid (n = 5/group). All data are presented as the mean ± SD. *$P < 0.05$ (unpaired *t*-test (A-E) or one-way analysis of variance followed by Tukey's multiple comparisons test (F)). IL-1β: Interleukin-1 beta; IL-6: interleukin-6; MPTP: 1-methyl-4-phenyl-1,2,3,6-tetrahydropyridine; n.s.: no significance; NaA: sodium acetate; QPCR: quantitative polymerase chain reaction; TH: tyrosine hydroxylase; TNF-α: tumor necrosis factor alpha.

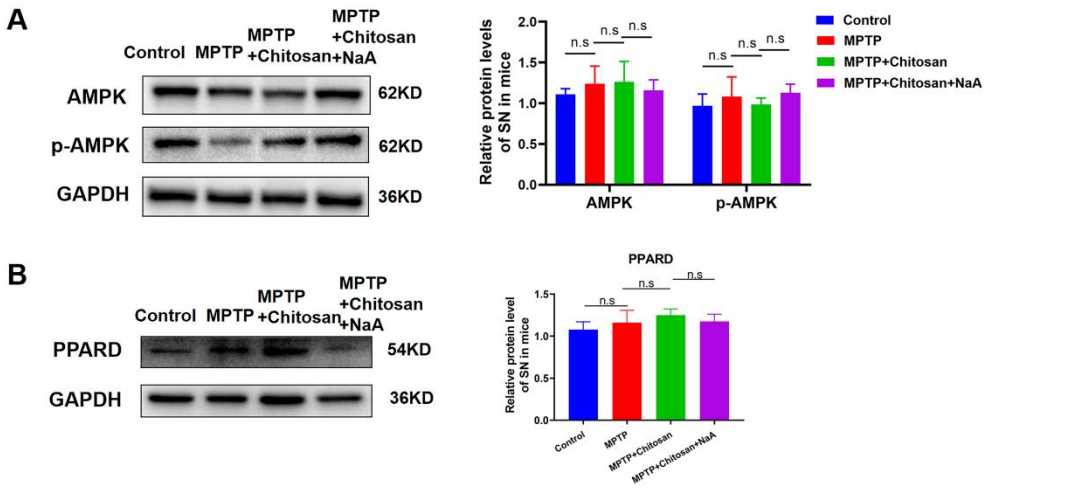

Additional Figure 3 The protein expression levels of PPARD and p-AMPK are unchanged in the substantia nigra with different treatment.

(A, B) Western blot analysis of AMPK, p-AMPK and PPARD protein expression levels in the mice of substantia nigra. GAPDH was used as loading control. All data were presented as the mean ± SD (n = 3/group). All experiments were repeated three times. **P* < 0.05 (one-way analysis of variance followed by Tukey's multiple comparisons test). AMPK: Adenosine 5'-monophosphate-activated protein kinase; GAPDH: glyceraldehyde-3-phosphate dehydrogenase; n.s.: no significance; NaA: sodium acetate; p-AMPK: phosphorylation adenosine 5'-monophosphate-activated protein kinase; PPARD: peroxisome proliferator-activated receptor delta.